Functional redundancy buffers plant communities against climate-driven shifts in composition

Irene Martín-Forés[1,2∓]*, Rhys V. Morgan[3∓], Samuel C. Andrew[4], Rachael V. Gallagher[5], Greg R. Guerin[1]

[1]School of Biological Sciences, The University of Adelaide, Adelaide, South Australia 5005, Australia

[2]TERN – Terrestrial Ecosystem Research Network, The University of Adelaide, Adelaide, Australia

[3]Department for Environment and Water (DEW). South Australian State Government

[4]CSIRO Agriculture & Food, Canberra, Australian Capital Territory, Australia

[5]Hawkesbury Institute for the Environment, Western Sydney University, Richmond, New South Wales, Australia

[∓] These authors contributed similarly.

*Corresponding author: irene.martin@adelaide.edu.au

Abstract

Climate change threatens plant communities worldwide with significant species losses, yet the consequences of reduced diversity for ecosystem function remain uncertain. Functional redundancy—where multiple species fulfill similar ecological roles—may act as 'functional insurance' by buffering ecosystem processes against species loss. Here, we combined plant composition data from 646 TERN AusPlots with gap-filled trait data (i.e. maximum plant height, leaf mass per area, and seed dry mass) from the AusTraits database to provide the first continental-scale assessment of functional redundancy in Australian plant communities. We estimated the potential impact of species losses under future climates based on community thermal and aridity tolerances relative to projected climate exposure. We examined the continental distribution of functional redundancy (in terms of competitive ability, resource acquisition strategies, and dispersal-establishment trade-offs in reproductive strategy), projected climate-driven compositional changes, and their relationship to bioclimate to identify vulnerable native communities.

Our results revealed strong latitudinal gradients of climate-change impacts on Australian plant communities, with those in the tropical north exposed to greater threat of changes in community composition because of future hotter and drier conditions not being unsuitable for monsoon-dependent species. Functional redundancy increased toward central Australia, aligning with more stressful (hotter, drier) bioclimates. At the biome scale, Mediterranean and arid communities showed higher functional redundancy and lower climate risk due to functional similarity in drought-adapted traits. Future rainfall changes were the dominant driver of climate-induced shifts in plant community composition.

The most vulnerable communities—at highest risk of functional destabilisation—were located along the northern coastline, with additional hotspots in the southernmost parts of the Mediterranean regions of South Australia and Western Australia. Conservation and monitoring efforts should prioritise these areas. Our findings highlight the influence of local bioclimatic factors on functional redundancy and the need to understand these dynamics to better forecast ecosystem resilience under ongoing climate change, while providing a spatial framework to guide biodiversity monitoring, policy, land management and conservation action across the Australian continent.

Keywords: community ecology; climate change; climate risk; ecosystem function; functional traits; functional redundancy; resilience; species loss; vulnerability.

1. Introduction

In the global context of rapid environmental change under widespread threatening processes such as climate change, land use change, and biological invasions (Valladares *et al.* 2019), there is an urgent need to protect biodiversity and better understand its role in the functioning of ecosystems (Díaz *et al.* 2019; Pettorelli *et al.* 2021). By providing a range of functional traits —measurable attributes or characteristics of species which relate to their fitness and ecological role on ecosystem processes (Gallagher *et al.* 2020)— biodiversity affects ecosystem functioning, productivity, resilience, and stability through complementary and overlapping ecological roles. In this sense, functional redundancy (F_R) measures the overlap in functional roles; it asserts that within an ecological community there may be functionally analogous species which contribute similar ecological roles to the functioning of an ecosystem (Walker, 1992). Thus, if one or more of these species becomes locally extinct or declines considerably, the remaining functionally analogous species will compensate for this loss and the net impact

on ecosystem function will be minimal (Walker, 1995). Consequently, higher F_R is predicted to enhance the resilience of ecosystems in terms of functional stability in the face of perturbation or species loss, while low F_R may indicate a lack of ecological resilience. Recent discussion has highlighted that the term redundancy may overstate substitutability, with some authors advocating for the broader concept of functional similarity instead (Eisenhäuer *et al.*, 2023). Here, we retain the F_R framework due to its ecological and conservation relevance in illustrating that certain species can be lost within a community without immediate loss of ecosystem functioning (Fischer and de Bello 2023); however, we acknowledge that it represents one end of a continuum of functional overlap among species, better conceptualised as functional similarity—a spectrum of overlapping but non-identical contributions to ecosystem processes (Eisenhauer *et al.* 2023).

Functional redundancy is intricately linked to other biodiversity metrics within plant communities, namely species diversity (S_D) and functional diversity (F_D) (Ricotta *et al.* 2016). Species diversity summarises the variety and abundance of taxonomically distinct organisms occurring in ecological communities, whereas F_D summarises the spread of functional traits within a community. Species-rich communities (high S_D) often have more species that can perform similar ecological roles, thus increasing the likelihood of functional redundancy (Fonseca and Ganade, 2001). Higher F_D indicates a wide array of ecological functions, being therefore widely considered to reflect overall ecosystem functioning (Cadotte *et al.* 2011). Functional redundancy provides a more mechanistic link between biodiversity and ecosystem resilience and stability; in the event of S_D loss, higher F_R should buffer a community from losing F_D, as the likelihood of losing a functionally unique species is reduced. Despite the growing interest in understanding how F_R affects ecosystem resilience (Biggs *et al.* 2020), how F_R varies at macroecological scales, and the potential drivers of such variation remain understudied.

Climate change has driven local and global species extinctions in deep time and is predicted to be a driver of plant extinction in the Anthropocene (Valladares *et al.* 2019). This loss of biodiversity is likely to impair the biological, chemical, and physical processes performed by ecosystems with the specific functional implications of such species loss only beginning to be understood (Hooper *et al.* 2012; Gallagher *et al.* 2013). Increasing temperature and changes in precipitation patterns, with subsequent changes in the frequency and duration of drought conditions, are likely to force many plant species beyond their climatic tolerance limits and towards extinction (Lancaster & Humphreys, 2020; Bennett et al. 2021). Assessing the vulnerability of different ecosystems to the effects of climate change has become a common

practice (Li *et al.* 2018). However, estimates of climate change vulnerability tend to focus on predicted changes to mean climate conditions and the direct impact these will have on species, while ignoring potential resilience mechanisms including individual physiological adaptation/tolerances and community level resilience mechanisms. Gallagher *et al.* (2019) addressed this limitation by measuring the adaptive capacity of Australian vegetation alongside a climate change risk metric (in the sense of projected climate-driven changes in community composition when the environmental niche limits are expected to be surpassed under future climate conditions). We propose that understanding F_R across Australia will also provide complementary information to the impact caused by climate change by indicating the functional resilience of plant communities to species loss. At present, the F_R in Australian plant communities has only been explicitly measured once as part of a global meta-analysis (Laliberté *et al.* 2010). More broadly, continental-scale functional trends and their environmental drivers have seldom been quantitatively investigated in Australian vegetation (Andrew *et al.* 2021, 2025).

Given the potential importance of F_R as an indication of community resilience to climate change induced species loss, our study seeks to achieve four main aims. These are to (1) determine the geographic distribution of F_R among plant communities across the Australian continent, (2) investigate how F_R varies along bioclimatic gradients, (3) map Australian communities that are most vulnerable to climate change by integrating species' exposure to projected climatic shifts with their sensitivity and adaptive capacity, and (4) examine the relationship between F_R and projected climate driven changes in the composition of sampled plant communities. Specifically, we hypothesised that (1) many locations across Australia would have very low F_D coupled with very high F_R (Andrew *et al.* 2021), due to species niche specialisation driven the continent's diverse and often extreme environmental gradients. Although the direction of the relationship between F_R and bioclimatic variables is unclear in terrestrial plant communities, we expect (2) F_R to be higher in more consistently extreme conditions (*e.g.* increased aridity), where species display drought- and heat-adaptive traits and therefore might be more similar functionally, and overlap more in their strategies evolved as long-term adaptations to persistent environmental stress. Based on the findings of Gallagher *et al.* (2019), we expect (3) the projected climate driven changes in composition not to be evenly distributed across Australia's plant communities, but reflect instead distinct geographic drivers; specifically, we expect temperature-driven changes to be most acute in the hotter northern regions, and precipitation-driven risks most pronounced in Mediterranean-type ecosystems of southwest Western Australia and southern South Australia. We expect these patterns assuming

that many species in these areas may already be close to their thermal or hydric limits, and therefore shifts could occur if communities overpass their limit threshold, regardless of their current F_R. Finally, we expect (4) F_R to be positively associated with projected climate-driven shifts in community composition, particularly in areas expected to become more arid, due to the synergistic effects of increasing heat and drought.

2. Methods

To achieve these aims we combined estimates of F_R with projected climate-driven changes in composition across an existing continental-scale plot network monitoring Australian plant communities. We measured F_R using the three traits of the leaf-height-seed (LHS) scheme which reflects the major axes of plant function: leaf mass per area (LMA), maximum plant height and seed dry mass (Westoby, 1998; Díaz *et al.* 2016). Leaf mass per area (LMA), the inverse of specific leaf area (SLA), captures species' trade-off between carbon investment in leaf-level photosynthetic tissues and leaf longevity (Westoby, 1998; Wright *et al.* 2004). Maximum plant height reflects species' strategies in relation to competition for light and is therefore related to canopy structure and shading in ecosystems (Westoby, 1998; Falster and Westoby, 2003). Seed dry mass indicates species' maternal investment in reproduction and can be related to the capacity to establish across different environmental niches (Westoby, 1998). Afterwards, we measured the climate change risk of individual species based on their observed climatic niches and then scaled this up to the community level by calculating the community weighted mean climate change risk (Gallagher *et al.* 2019), and we mapped F_R and climate change risk to determine their spatial distributions. Finally, we constructed linear regression models to explore the relationship between F_R, climate change risk and environmental variables.

We combined plant community composition data, species functional trait data, long-term climate data, predicted climate change exposure data and species climate niche data to generate our response and predictor variables. The continental approach enables broadscale trends to be detected along key bioclimatic gradients such as temperature and precipitation, elucidating environmental drivers of community-level properties such as F_R and climate change risk (Violle *et al.* 2014). Furthermore, the Australian continental flora is a particularly useful study system due to the contrasting climates existing across the land, that strongly influence species distribution, and the characteristics of the different ecosystems (Hughes *et al.*, 2003; Keith 2017). Australia is latitudinally characterised by a tropical north with wet summers and dry winters, an arid to semi-arid interior covering most of the continent, and a

166 temperate south with hot dry summers and cool wet winters (Keith 2017). Apart from
167 analysing these trends at the continental scale, to detect scale-dependency in our results we
168 also conducted the analyses at two finer spatial scales. First, we replicated the analyses at the
169 biome scale, using the Ecoregion 2017 dataset based on the classification provided by Olson
170 *et al.* (2001) which designates 7 major biomes in Australia.
171
172 ***2.1. Plant community composition data***
173 The Terrestrial Ecosystem Research Network (TERN) AusPlots ecosystem surveillance
174 program monitors over 1,000 1-ha plots across the Australian continent (Fig. 1) (Sparrow *et al.*
175 2020). The network is stratified by bioregion to maximise ecological coverage (Guerin *et al.*
176 2020a). All plots are systematically surveyed using a point-intercept method comprising a grid
177 of 1,010 points which yields robust estimates of species percent cover (White *et al.* 2012). A
178 specimen is collected from each recorded species and herbarium determinations are obtained
179 for all specimens, thus ensuring taxonomically sound data. We extracted plot-level vascular
180 plant species percent cover data for 787 TERN AusPlots using the 'ausplotsR' package (Guerin
181 *et al.* 2020b; Munroe *et al.* 2021). In cases where repeated surveys were available for plots, the
182 most recent survey was selected to ensure that the data best reflected current species
183 composition. We used species percent cover data as a proxy for species relative abundances.
184 For analyses at continental-scale we modelled all plots across the TERN AusPlots
185 network together. For biome-scale analyses we grouped plots according to the major biome
186 they occupy in the Olson *et al.* (2001) biome classification (Fig. 1). From analyses at the biome
187 scale, we selected four biomes, including temperate broadleaf and mixed forests (biome 4),
188 tropical/subtropical grasslands, savannas and shrublands (biome 7), Mediterranean forests,
189 woodlands and shrublands (biome 12), and deserts and xeric shrublands (biome 13). Other
190 biomes present in Australia (i.e. biome 1 - Tropical/Subtropical Moist Broadleaf Forests, biome
191 8 - Temperate Grasslands, Savannas & Shrublands and biome 10 - Montane Grasslands &
192 Shrublands) were excluded from this study due to the low number of TERN AusPlots within
193 their boundaries. These four biomes object of study capture the major climatic and ecological
194 gradients in Australian vegetation. Tropical and subtropical grasslands, savannas, and
195 shrublands (biome 7) are characterized by high mean annual temperatures, strong seasonality
196 in rainfall, and dominance of fire- and drought-adapted species, often occupying narrow
197 ecological niches (Shaw *et al.* 2000). Temperate broadleaf and mixed forests (biome 4), in
198 contrast, experience moderate temperatures and relatively stable precipitation, supporting
199 higher species richness and less extreme functional constraints (Bailey, 1964). Mediterranean

forests, woodlands, and shrublands (biome 12) in southwestern and southeastern Australia are shaped by hot, dry summers and mild, wet winters, favouring species with stress-tolerant or drought-avoidance strategies (Lionello *et al.* 2006). Deserts and xeric shrublands (biome 13) are characterized by extremely low precipitation, high temperatures, and high climatic variability, resulting in plant communities strongly constrained by environmental filtering (Noy-Meir, 1973). Grouping plots by these biomes allows us to assess context-specific functional responses, capturing how climate, species physiology, and evolutionary history interact to shape diversity and functional redundancy across contrasting environmental settings (Laliberté *et al.* 2010).

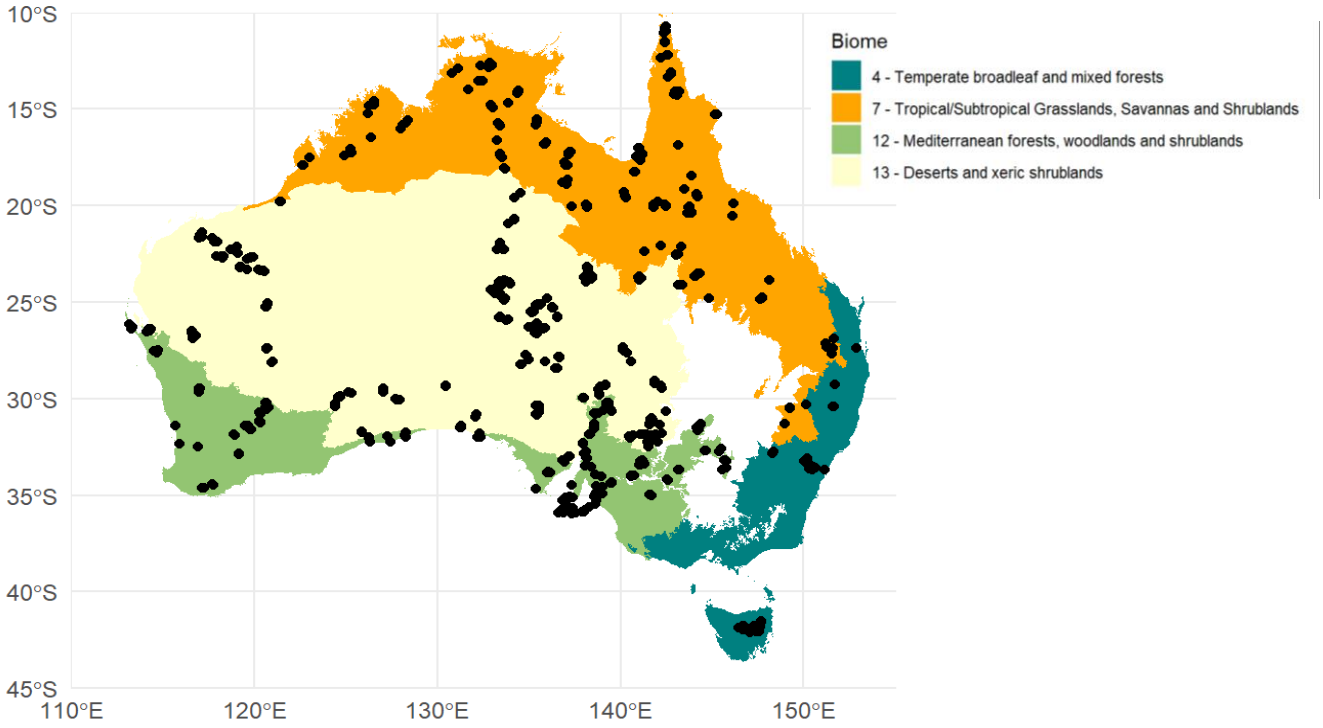

Figure 1. Biomes of Australia used in this study and geographic locations of AusPlots flora inventories (black circles). Biome 4 – Temperate broadleaf and mixed forests (n = 43 plots), biome 7 – Tropical/Subtropical Grasslands, Savannas & Shrublands (n = 218 plots), biome 12 - Mediterranean Forests, Woodlands & Shrublands (n = 203 plots), biome 13 - Deserts & Xeric Shrublands (n = 280 plots). Note that several biomes were excluded from this study due to the low number of TERN AusPlots within their boundaries: biome 1 - Tropical/Subtropical Moist Broadleaf Forests (n = 0), biome 8 - Temperate Grasslands, Savannas & Shrublands (n = 28) and biome 10 - Montane Grasslands & Shrublands (n = 15).

2.2. Trait data

We extracted trait data from the AusTraits database 6.0.0 for all species occurring in our plots. AusTraits contains data for 448 functional traits across 28,640 Australian taxa compiled from multiple sources (Falster *et al.* 2021).

From the 4,428 species recorded in AusPlots with the point intercept methodology, we obtained mean values for maximum plant height (3,641 species), leaf mass per area (LMA) (1,304 species), and seed dry mass (2,574 species), respectively. We log transformed all trait values to account for differences in their units and skewness in their distributions, which is standard for community trait analysis (Bruelheide *et al.* 2018). To improve species representation, we followed the methods outlined in Andrew *et al.* (2021), consisting of two subsequent steps by which missing trait values were first estimated missing values via linear models, and subsequently gap-filled utilising all accessible and relevant trait data from the native Australian flora. In summary, to leverage the available measurements of leaf/phyllode and seed dimensions for a significant proportion of species in AusTraits, we first estimated leaf area for species lacking direct area measurements based on measurements of leaf length and width. To do so, we conducted Linear Mixed Models (LMM) using the lme4 R package (Bates 2010). Likewise, seed dry mass was estimated using seed length as a fixed effect, combined with a random factor of family. Predicted trait values were well correlated to known values (seed mass $r^2 = 0.85$, leaf area $r^2 = 0.81$). The models demonstrated strong explanatory power, evidenced by high conditional R^2 values (R^2_c) for both trait models, with a substantial portion of the explanatory power derived from fixed effects, reflected in high marginal R^2 values (seed dry mass: $R^2_c = 0.85$; $R^2_m = 0.68$; leaf area: $R^2_c = 0.79$; $R^2_m = 0.66$).

We adopted a minimum threshold of 80% trait coverage by abundance for plots to be included in our study as this threshold has been shown to limit the estimation bias of community weighted functional properties (Borgy *et al.* 2017). In a second step, to increase the taxonomic coverage of trait data we gap-filled values for species without direct observations in AusTraits using the GapFilling() function from the BHPMF R package (Schrodt *et al.*, 2015), which employs Bayesian hierarchical probabilistic matrix factorisation and correlation structure to impute missing trait values. This method exploits trait–trait correlations and phylogenetic trait signals within the existing trait data to predict unknown trait values. Gap-filling was run on a matrix of trait values for plant height, leaf area, length, and width, leaf mass per area (inverse of SLA), and seed mass and length; species with no available trait data were dropped from all subsequent analyses (n = 24,915 native Australian plant species retained). Finally, we applied the 80% trait coverage by abundance threshold to the total of 787 AusPlots, leaving 649 plots which met the threshold.

2.3. Diversity indices

We calculated four diversity indices, including species richness (S_R), species diversity (S_D), functional diversity (F_D) and functional redundancy (F_R). We followed the methodology of Ricotta *et al.* (2016) in which S_D is calculated as Simpson's diversity index and F_D is calculated as Rao's quadratic entropy. Simpson's diversity is bound between 0 and 1 and it incorporates plot-level species relative abundances. Rao's quadratic entropy is also bound between 0 and 1 and it accounts for plot-level species relative abundances as well as species pairwise functional dissimilarities. Rao's quadratic entropy is ultimately the mean functional dissimilarity of two randomly selected individuals from a given community (Botta-Dukát, 2005). Importantly, the maximum value of Rao's, when all species are maximally functionally dissimilar, is equal to Simpson's index. Therefore, dividing S_D by F_D yields a measure of the functional uniqueness of a community (U).

$$U = \frac{F_D}{S_D} \qquad \text{(eq. 1)}$$

The complement of U is a measure of the functional redundancy of a community (F_R), which summarises the proportion of species diversity not encompassed by functional diversity.

$$F_R = 1 - U \qquad \text{(eq. 2)}$$

All alpha diversity indices were computed with the 'uniqueness' R function provided by Ricotta *et al.* (2016).

To assess whether F_R exhibited any statistically detectable geographic structure, we quantified spatial autocorrelation using Moran's I with a 5-nearest-neighbour spatial weights matrix. In addition, we evaluated broad spatial trends by modelling F_R as a function of latitude and longitude (second-order polynomial terms). To assess whether F_R differs among major Australian biomes, we also conducted a one-way ANOVA with subsequent Tukey HSD post-hoc tests to evaluate pairwise differences among biomes.

2.4. Bioclimatic data

We obtained long term (1970-2000) mean climate data in a raster format from 'WorldClim 2.1' and extracted values at the coordinates of each plot (Fick and Hijmans, 2017) at a resolution of 10 minutes of a degree. We extracted mean annual temperature (MAT; °C), temperature annual range (T-Range; °C), maximum temperature of the warmest month (T-Max; °C), mean annual precipitation (MAP; mm), precipitation seasonality (P-Seasonality) and precipitation of the driest month (P-Dry; mm). These variables reflect the mean, variability, and extremes of

temperature and precipitation, all of which are projected to change under future climate scenarios for Australian ecosystems (Hughes, 2003).

2.5. Future climate projections and climate change risk

To assess the climate change risk faced by plant communities across Australia, we followed an approach informed by Gallagher *et al.* (2019), by adapting their grid-based methodology in order to calculate plot-based climate change risk metrics. We calculated metrics of risk for changes to both MAT and MAP. For these calculations we used the same set of species as in the diversity index calculations to enhance comparability between diversity indices and climate change risk metrics. First, we obtained species-level climate niche data compiled by Gallagher *et al.* (2019), which represents the realised climatic limits of Australian plant species based on cleaned occurrence records for herbarium specimens from the Australian Virtual Herbarium (AVH). To account for potential outliers in these occurrence records, we defined species' temperature tolerance (MAT tolerance) as the 98th percentile of mean annual temperature (MAT) values across their distribution, and precipitation tolerance (MAP tolerance) as the 2nd percentile of mean annual precipitation (MAP) values. We then matched these species-level climate tolerances to the species occurring in each plot and calculated community-weighted mean (CWM) climate tolerances by multiplying each species' tolerance value by its relative abundance in the plot. These CWMs represent the average climatic tolerance of the plant community in terms of upper temperature and lower precipitation limits.

To assess current climatic safety margins, we subtracted the present-day (baseline) climate conditions from the community-weighted mean tolerance values at each plot. Specifically, for MAT and MAP, the safety margins were, respectively, calculated as:

$$MAT\ Safety\ Margin = CWM\ MAT\ Tolerance - Current\ MAT$$

$$MAP\ Safety\ Margin = Current\ MAP - CWM\ MAP\ Tolerance$$

These safety margins represent the climatic buffer a plant community has before it reaches its collective thermal or drought limit.

Australia is projected to experience substantial warming by 2070, with mean annual temperatures expected to increase across the continent, particularly in the interior and northern regions. Precipitation patterns are likely to become more variable, with decreases in cool-season rainfall and longer drought duration projected for many parts of the south and east (especially mediterranean-type regions), while some northern areas may experience more intense wet-season rainfall events (State of the Climate 2024). Hence, we then estimated future

climate exposure by calculating projected changes in MAT and MAP between current climate conditions and predicted projections for 2070 under the high-emissions scenario RCP8.5 (rcp85, 800 ppm of CO_2 by 2070). For that, we used downscaled climate data from CHELSA based on five global circulation models for 2061-2080, including ACCESS1.0, CNRM-CM5, HADGEM2-CC, MIROC5, and NorESM1-M.

Finally, we calculated plot-level climate change risk as the difference between exposure and safety margin:

$$MAT\ Risk = Exposure - Safety\ Margin$$

$$MAP\ Risk = -\ (Exposure - Safety\ Margin)$$

For MAT, a positive risk value indicates that future climate change by 2070 in terms of temperature is expected to exceed the current adaptive capacity of the community (i.e. the community's mean tolerance limit), placing it at greater risk. Conversely, negative or low risk values suggest that the community's climatic buffer is sufficient to accommodate projected temperature changes. For MAP, the opposite, when Exposure − Safety Margin has a negative value indicates that future drought conditions by 2070 are expected to exceed the current adaptive capacity of the community, placing it at greater risk, whereas positive values suggest that the community's climatic buffer is sufficient to accommodate projected temperature changes, hence why the values have been multiplied by (-1).

We acknowledge that species respond individually to climate change and that communities are not strictly discrete units. Community-weighted mean (CWM) tolerances provide an operational estimate of the average climatic tolerance of the dominant species in each plot, capturing the functional response of the community as a unit. While individual species may exceed their limits without immediately altering functional diversity, CWM-based safety margins allow meaningful comparison of climate change risk across plant communities.

2.6. Mapping alpha functional redundancy and climate change risk

To visualise the spatial distribution of F_R and climate change risk we created maps depicting their values across the TERN AusPlots continental network using the ggplot2 (Wickham 2016) and ggpmisc (Aphalo 2025) packages in R. We generated separate maps for MAT Risk, MAP Risk and alpha F_R. Additionally, we constructed bivariate maps –derived directly from quantitative, plot-level metrics, ensuring that observed patterns reflect measured differences rather than subjective interpretation– which illustrates F_R and climate change risk simultaneously for each plot. For mapping functional redundancy (F_R) and climate change risk

(MAT and MAP), we classified plots into three categories each. F_R categories were defined as follows: low redundancy corresponded to the lowest 33% of F_R values, medium redundancy included values between the 33rd percentile and the median of plots considered at risk, and high redundancy included values above that median. MAT Risk was classified as low risk for plots that were not at risk (MAT Risk < 0); similarly, MAP Risk was classified as low risk for plots that were not at risk (MAP Risk > 0). Among plots at risk (MAT Risk ≥ 0 and MAP Risk ≤ 0), we then used the median of the at-risk subset to distinguish medium and high risk categories. approach ensures that the classification reflects both the distribution of F_R and the degree of climate change exposure among at-risk plots, avoiding the bias introduced by equal-interval or quartile-based splits of the entire dataset. Beyond serving as a visual illustration, these bivariate maps provide an analytical framework to identify spatial patterns and hotspots of vulnerability, (high climate change risk and low F_R), highlighting plots that will likely undergo climate-driven changes in community composition and enabling comparison across regions and prioritisation for conservation or further study.

2.7. Modelling the relationship between diversity indices, bioclimate and climate change risk

We investigated the drivers of plant diversity metrics (species richness, S_R; species diversity, S_D; functional diversity, F_D; functional redundancy, F_R) and climate-driven vulnerability (MAT Risk, MAP Risk) using linear regression models at two spatial scales: continental (all AusPlots across Australia) and biome-specific. For diversity metrics, we included six bioclimatic predictors (MAT, T-Max, T-Range, MAP, P-Dry and P-Season). For climate risk metrics, we tested two complementary predictor sets: bioclimatic variables and diversity indices (S_R, S_D, F_D, F_R). All models were additive and excluded interactions. We evaluated all possible models containing any subset of predictors, including the null model, and selected the best-supported model based on the lowest Akaike Information Criterion (AIC). For each model, we calculated ΔAIC and Akaike weights, with ΔAIC < 2 indicating substantial support. From each best-supported model, we extracted slopes, standard errors, t-values, p-values, and goodness-of-fit metrics (R^2, adjusted R^2, residual standard error, AIC, BIC) to quantify the strength, direction, and significance of predictors. Only results from the best-supported models are reported.

3. Results

Species richness (S_R) averaged 21.01 species per plot (± 11.17 Standard Deviation (SD); Inter Quartile Range (IQR) = 13–27) , indicating high variability across the sampled sites. Species diversity (S_D) had a mean of 0.72 (± 0.18 SD; IQR = 0.64–0.85), while quadratic functional

diversity (F_D) averaged 0.18 (± 0.07 SD; IQR = 0.14–0.22). Functional redundancy (F_R) in sampled plant communities ranged from 0.44 to 0.93, with a mean value of 0.75 (± 0.07 SD; IQR = 0.71–0.80).

While no dominant spatial pattern for F_R was evident across the continent (Fig. 2), there was a tendency for higher F_R in the interior regions. In this sense, F_R showed significant positive spatial autocorrelation (Moran's I = 0.205, $p \leq 0.001$), indicating that nearby plots tend to be more similar in F_R than expected by chance. However, spatial position explained only a small proportion of variation (adjusted $R^2 = 0.048$) in the latitudinal–longitudinal model, suggesting that while spatial structure is present, geographic trends are weak and consistent with our description of broad tendencies rather than strong regional gradients. A linear regression of F_R against latitude revealed a slight positive relationship (slope = 0.00095, p = 0.020, $R^2 = 0.008$), indicating that F_R tends to increase slightly toward more northerly sites, although latitude alone explains very little of the overall variation. As such, central Queensland, the arid zones of South Australia and the Northern Territory, and parts of western New South Wales appeared as hotspots of high F_R. In contrast, regions such as Tasmania, eastern New South Wales, the west coast of Western Australia, the northern tip of the Northern Territory, and the Mount Lofty Ranges in South Australia exhibited mostly lower F_R values. When comparing F_R across biomes, we found significant differences (ANOVA: $F = 10.42$, $p \leq 0.001$). Pairwise comparisons (Tukey HSD) indicate that some biomes, including the arid deserts and xeric shrublands (biome 13) and the tropical and subtropical grasslands, savannas and shrublands (biome 7), had significantly higher F_R than Mediterranean-type (biome 12) and temperate forest (biome 4) biomes (see supplementary material for further details). Overall, plots with high F_R were not strongly spatially segregated from those with low F_R; thus, despite these broad-scale differences, high and low F_R plots remain intermixed locally, supporting our original conclusion that fine-scale hotspots (e.g., Central Queensland, Mount Lofty Ranges) reflect site-level variation that cannot be fully captured by biome aggregation.

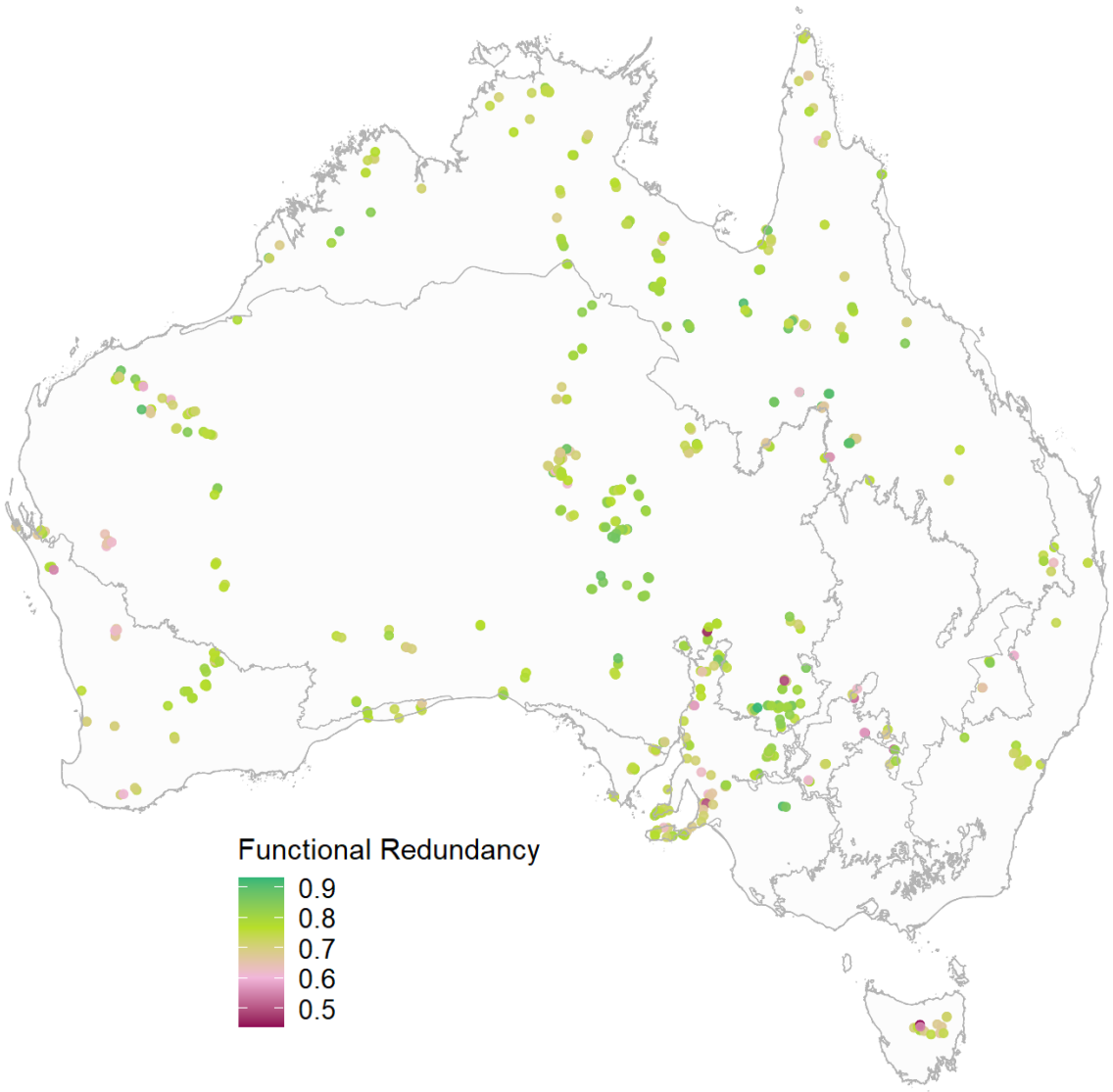

Figure 2. Map of plot-level functional redundancy values across the TERN continental vegetation monitoring plot network (n = 646; notice that for three plots, calculations of certain diversity metrics were not possible). Colour denotes functional redundancy (legend). The plant communities in highly redundant plots (dark green) are expected to maintain stable ecosystem functioning in the event of species loss. The plant communities in plots with low functional redundancy values (dark pink) are expected to experience unstable ecosystem functioning in the event of species loss. Black lines indicate the approximate boundaries of major Australian biomes, providing geographic context for the distribution of functional redundancy values.

3.1. Variation of diversity indices along bioclimatic gradients

While some temperature variables were correlated (e.g., MAT and T-Max, $r = 0.87$, $p \leq 0.001$; see supplementary material for further details), we show their independent bivariate relationships to illustrate the different ecological dimensions of each bioclimatic variable.

Across Australia, multivariate AIC-selected models revealed consistent and strong climatic controls on plant diversity patterns. Species richness (S_R), species diversity (S_D), and functional diversity (F_D) were primarily shaped by temperature–precipitation trade-offs, with MAT exerting predominantly negative effects and MAP showing positive or stabilizing influences (Table 1). In particular, at the continental scale, S_R decreased with MAT and T-Range and increased with MAP and P-Season. S_D and F_D were negatively influenced by MAT and P-Dry and positively influenced by MAP (and T-Max in the case of F_D). Together, these models explained between 7% and 24% of the variation in S_R, S_D, and F_D. In contrast, functional redundancy (F_R) responded only weakly to climate. F_R increased with MAT and T-Range and decreased with T-Max and P-Season. Although several predictors were retained in the best model for F_R, this only explained 4% of its variation, indicating that functional redundancy seems to be decoupled from broad-scale climatic gradients.

Biome-level patterns revealed substantial regional differentiation in climatic drivers. In temperate broadleaf and mixed forests (biome 4), S_R increased with T-Max and decreased with T-Range, which also affected F_D negatively. However, S_D was determined by precipitation variables, with MAP having a positive effect and P-Dry and P-Season a negative one. In tropical and subtropical grasslands, savannas and shrublands (biome 7), S_R increased with MAT but declined with T-Max, P-Dry and P-Season, while S_D and F_D were most strongly and positively associated with MAP and negatively with P-Season; finally, F_R was positively influenced by T-Range. Mediterranean forests, woodlands and shrublands (biome 12) showed pronounced precipitation influences, with S_R, S_D and F_D all positively shaped by combinations of P-Dry and P-Season, alongside negative MAT effects for S_R and S_D. F_R in biome 12 was negatively affected by MAT, MAP and P-Dry. Finally, in deserts and xeric shrublands (biome 13), S_R was negatively affected by MAT, and T-Range and positively by T-Max and MAP; S_D was positively influenced by P-Season, whereas and F_D was negatively influenced by MAT, and positively by T-Max and P-Season. F_R in biome 13 was positively influenced by MAT, and negatively by T-Range, MAP, and P-Season. These contrasting results across biomes indicate that diversity metrics respond to different climatic dimensions depending on regional environmental context.

While we do not present ordinations of species or trait composition here, the distinctness of biomes and habitats can be explored using the species and trait data available through the 'ausplotsR' package (Guerin *et al.* 2020b; Munroe *et al.* 2021).

Table 1. Best-fit linear models explaining spatial variation in species richness (SR), species diversity (SD), functional diversity (FD), and functional redundancy (FR) across Australia and within selected biomes. Models were selected using AIC-based stepwise selection. The table reports the retained predictors, model fit statistics (R^2, adjusted R^2, sigma), and information criteria (AIC, BIC). The direction and statistical significance of each predictor in the best model are shown in brackets after each term (+: positive effect; –: negative effect; * $p \leq 0.05$, ** $p \leq 0.01$, *** $p \leq 0.001$). Predictors without brackets were retained in the best model but were not statistically significant.

Response Variable	Best model formula	R^2	Adj R^2	sigma	AIC	BIC	$df_{residual}$
The whole Australia – All AusPlots							
S_R	SR ~ MAT$^{(-***)}$ + T_Max $^{(+***)}$ + T_Range$^{(-***)}$ + MAP$^{(+***)}$ + P_Season$^{(+*)}$	0.24	0.23	9.75	4783.56	4814.85	640
S_D	SD ~ MAT$^{(-***)}$ + MAP$^{(+***)}$ + P_Dry$^{(-***)}$	0.08	0.07	0.08	-434.38	-434.02	642
F_D	FD ~ MAT$^{(-***)}$ + T_Max $^{(+*)}$ + T_Range + MAP$^{(+***)}$ + P_Dry$^{(-**)}$	0.11	0.11	0.11	-1764.83	-1733.54	640
F_R	FR ~ MAT$^{(+***)}$ + T_Max$^{(-**)}$ + T_Range$^{(+**)}$ + MAP + P_Season$^{(-*)}$	0.04	0.04	0.04	-1566.12	-1534.83	640
Biome 4 – Temperate broadleaf and mixed forests							
S_R	SR ~ T_Max$^{(+***)}$ + T_Range$^{(-***)}$	0.57	0.54	8.30	231.10	236.96	29
S_D	SD ~ MAT + MAP$^{(+**)}$ + P_Dry$^{(-*)}$ + P_Season$^{(-*)}$	0.31	0.21	0.16	-18.81	-10.01	27
F_D	FD ~ T_Range$^{(-*)}$	0.17	0.14	0.06	-84.79	-80.39	30
F_R	FR ~ MAT	0.06	0.03	0.07	-72.10	-67.70	30
Biome 7 – Tropical / subtropical grasslands, savannas and shrublands							
S_R	SR ~ MAT$^{(+***)}$ + T_Max$^{(-***)}$ + P_Dry$^{(-**)}$ + P_Season$^{(-***)}$	0.31	0.29	9.91	1291.47	1310.39	168
S_D	SD ~ MAT + MAP$^{(+***)}$ + P_Season$^{(-*)}$	0.13	0.12	0.17	-114.92	-99.15	169
F_D	FD ~ MAP$^{(+***)}$ + P_Season$^{(-*)}$	0.14	0.13	0.06	-473.37	-460.76	170
F_R	FR ~ T_Range$^{(+*)}$	0.04	0.03	0.07	-431.87	-422.41	171
Biome 12 – Mediterranean forests, woodlands and shrublands							
S_R	SR ~ MAT$^{(-***)}$ + T_Max$^{(+**)}$ + P_Dry$^{(+***)}$ + P_Season$^{(+*)}$	0.50	0.48	8.30	1201.84	1220.62	164
S_D	SD ~ MAT$^{(-**)}$ + P_Season$^{(+***)}$	0.17	0.16	0.15	-165.96	-153.44	166
F_D	FD ~ P_Dry$^{(+***)}$ + P_Season$^{(+***)}$	0.21	0.21	0.06	-489.30	-476.78	166

F_R	$FR \sim MAT^{(-***)} + MAP^{(-***)} + P\_Dry^{(-***)}$	0.20	0.18	0.07	-433.99	-418.34	165
Biome 13 – Deserts and xeric shrublands							
S_R	$SR \sim MAT^{(-***)} + T\_Max^{(+**)} + T\_Range^{(-*)} + MAP^{(+***)}$	0.11	0.09	8.25	1658.41	1679.14	229
S_D	$SD \sim P\_Season^{(+*)}$	0.02	0.01	0.17	-161.00	-150.63	232
F_D	$FD \sim MAT^{(-***)} + T\_Max^{(+***)} + MAP + P\_Season^{(+*)}$	0.08	0.06	0.06	-653.69	-632.96	229
F_R	$FR \sim MAT^{(+***)} + T\_Range^{(-***)} + MAP^{(-*)} + P\_Season^{(-**)}$	0.15	0.13	0.07	-605.50	-584.77	229

468

3.2. Geographic distribution of climate change risk and its relationship to environmental variables

Out of 649 plots, 201 (31%) are considered at risk to species turnover and changes in community composition due to projected changes in mean annual temperature (Risk MAT ≥ 0; Fig. 3). Plots with the highest Risk MAT values are primarily located in the northern half of the continent, whereas lower-risk plots occur at more southerly latitudes. Meanwhile, 608 plots (93.7%) are considered at risk from predicted changes in mean annual precipitation (Risk MAP ≤ 0), with the highest-risk plots generally located at the northern and southern extremes of the continent and lower-risk plots in central regions (Fig. 3). Across the TERN AusPlots network, regression analyses revealed that Risk MAT increases strongly with latitude ($R^2 = 0.58$, $p < 0.001$), indicating higher temperature-driven risk in northern regions (slope = 0.254 °C per decimal degree latitude; Fig. 3c). Incorporating longitude slightly improved model fit ($R^2 = 0.66$, $p < 0.001$), showing that risk rises northwards but decreases slightly westwards (longitude slope = -0.071 °C per decimal degree). In contrast, Risk MAP declines with latitude ($R^2 = 0.20$, $p < 0.001$), suggesting greater precipitation-driven risk in southern regions. These regression models complement the histograms and maps, quantitatively highlighting broad latitudinal trends in climate change exposure.

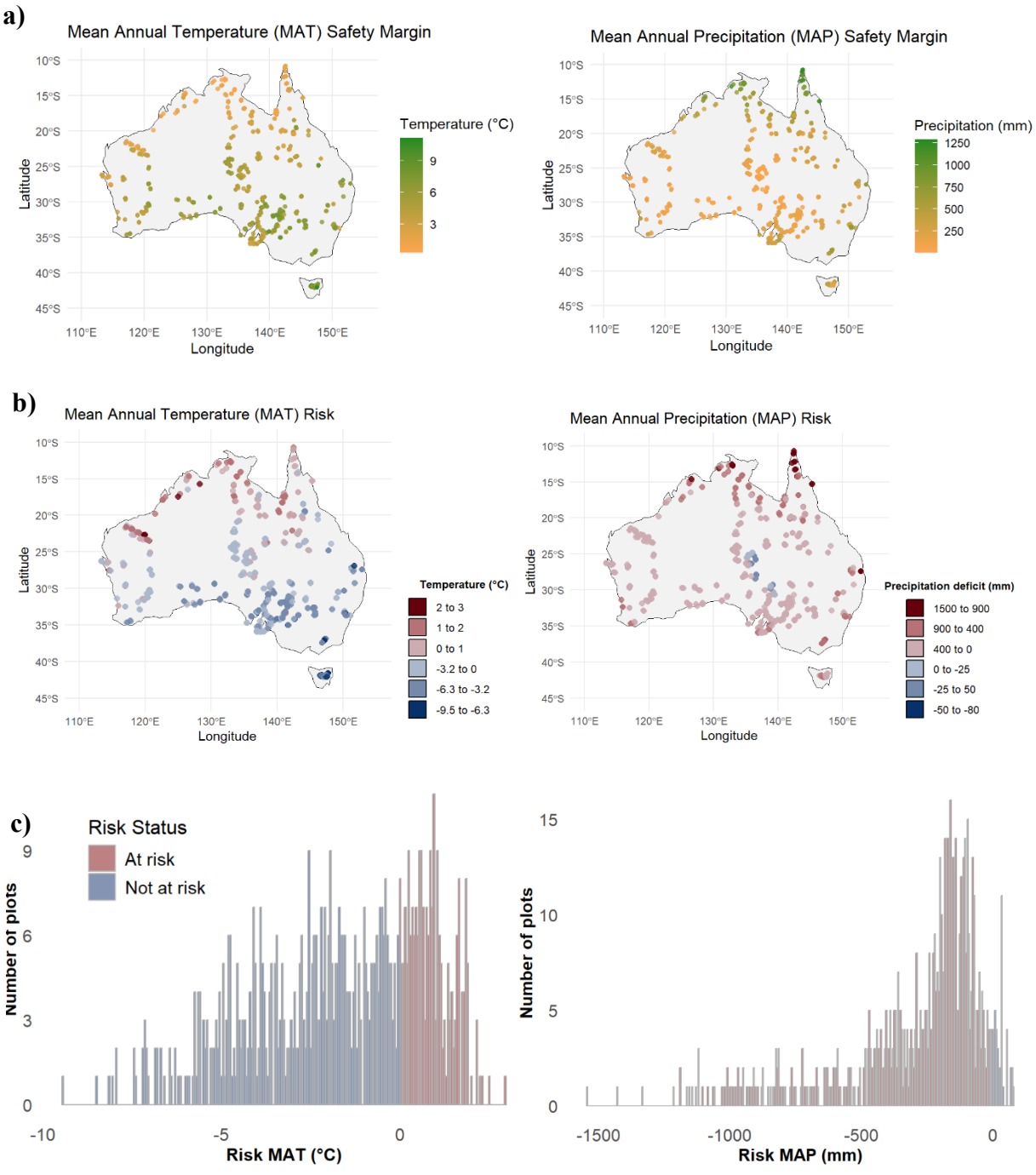
a)
Mean Annual Temperature (MAT) Safety Margin
Temperature (°C)
9
6
3
Mean Annual Precipitation (MAP) Safety Margin
Precipitation (mm)
1250
1000
750
500
250
Latitude
Longitude
10°S
15°S
20°S
25°S
30°S
35°S
40°S
45°S
110°E
120°E
130°E
140°E
150°E
b)
Mean Annual Temperature (MAT) Risk
Temperature (°C)
2 to 3
1 to 2
0 to 1
-3.2 to 0
-6.3 to -3.2
-9.5 to -6.3
Mean Annual Precipitation (MAP) Risk
Precipitation deficit (mm)
1500 to 900
900 to 400
400 to 0
0 to -25
-25 to 50
-50 to -80
c)
Risk Status
At risk
Not at risk
Number of plots
Risk MAT (°C)
Risk MAP (mm)
d)

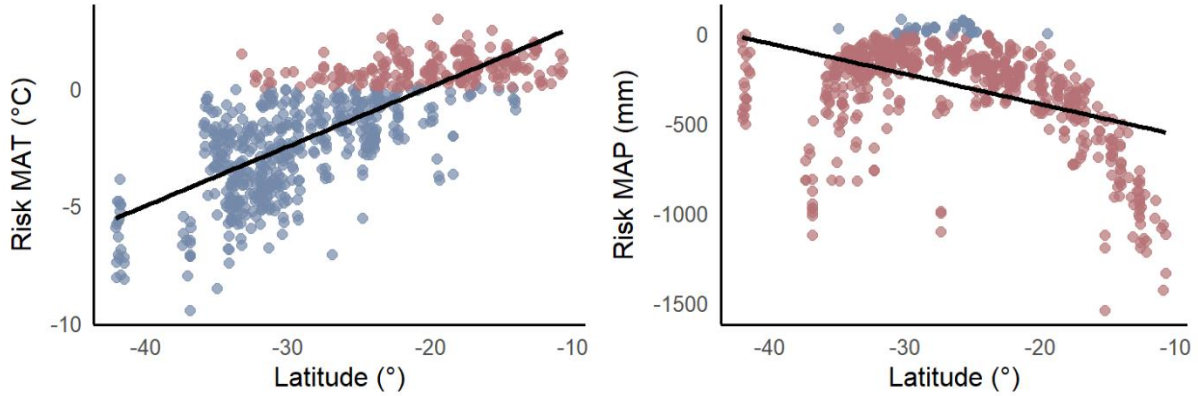

Figure 3. a) mean annual temperature (MAT) (left) and mean annual precipitation (MAP) (right) safety margins; **b)** climate change risk in terms of predicted changes to MAT (left) and MAP (right) across the TERN AuPlots network; **c)** distribution histograms of Risk MAT and Risk MAP; and **d)** scatterplots of Risk MAT and Risk MAP versus latitude with fitted linear regression lines (solid) and 95% confidence intervals (shaded), illustrating broad latitudinal trends in climate change exposure across the network. For MAT climate change risk, notice that the values in the legend represent °C, over (positive) or below (negative) the safety margin, to which the vegetation community will be exposed in the future. For MAP climate change risk, notice that the values in the legend represent water deficit, over (positive; i.e. more water deficit and harsher conditions) or below (negative) the safety margin, to which the vegetation community will be exposed in the future. Red points on the map represent at risk plots, while blue colours represent plots with risk values of zero or less (the darker the blue the less at risk). On the histograms, bars for plots at risk (positive for MAT, negative for MAP) are shown in red, while plots not at risk are shown in blue, highlighting the big proportion of plots at risk across the network.

Across all AusPlots, MAT Risk increased with higher T-max and P-season, and decreased with increasing MAT and temperature range (T-Range), indicating that sites in hotter regions with marked precipitation seasonality are projected to experience greater temperature-driven turnover (Table 2; see supplementary material for full model outputs). In contrast, MAP Risk increased with MAT, MAP, P-dry, and P-season, and decreased with T-range and T-max, suggesting that precipitation-driven turnover is highest in warm sites with moderate temperature variability (Table 2; Supplementary material). MAP Risk displayed an inverse patter, increasing with MAT and T-Range and decreasing with MAP and T-Max, with an additional negative effect of P-Dry. These patterns indicate that temperature-driven and

precipitation-driven turnover risks respond to distinct climatic axes, with the former most elevated in warmer and seasonal environments, and the latter being greater in hotter and arid regions.

At the biome scale, the relationships between MAT/MAP Risk and bioclimatic variables were quite contrasting for different biomes (Table 2; Supplementary material).In temperate forests (biome 4), MAT Risk increased with MAT, while MAP Risk was influenced by nearly all predictors, including positive effects of MAP and T-Max and negative effects of MAT, P-Dry, and T-Range (Table 2; Supplementary material). In tropical and subtropical savannas (biome 7), MAT Risk increased with MAT, P-Dry, and T-Range, whereas MAP Risk was primarily driven by precipitation (positive effect of MAP, although negative effect of and P-Season) and moderated by temperature variability (negative effects of T-Range, and a positive effect of T-Max). In Mediterranean systems (Biome 12), MAT Risk reflected the joint influence of temperature and seasonality, increasing with T-Max and P-Season, while MAP Risk was dominated by a strong positive effect of MAP and MAT and a negative effect of P-Season. In deserts and xeric shrublands (Biome 13), MAT Risk was elevated in warmer sites (positive effects of MAT and T-Max) and declined with P-Dry, while MAP Risk increased with MAP, T-Max, and P-Dry and declined with MAT.

3.3. Relationship between climate change risk and diversity metrics

At the continental scale, MAT Risk was not significantly associated with any of the diversity metrics (S_R, S_D, F_D, or F_R), indicating that variation in these community attributes does not strongly predict temperature-driven turnover. By contrast, MAP Risk exhibited a strong negative relationship with S_R, with communities containing more species showing lower precipitation-driven risk (Table 3; supplementary material).

At the biome scale, the influence of diversity metrics on climate change driven risk was more variable. For temperate forests (biome 4), no diversity metrics were significantly associated with MAT Risk, while MAP Risk decreased significantly with S_R. In tropical savannas (biome 7), MAT and MAP Risk increased with S_R. In Mediterranean systems (biome 12), MAT Risk was positively related to S_R, while MAP Risk increased with S_R but decreased with F_R, suggesting that communities with high redundancy buffer better precipitation-driven risk. In deserts (biome 13), MAT Risk increased with F_D but decreased with S_D, whereas MAP Risk showed a more complex pattern, increasing with S_R and F_D but decreased with S_D,

indicating that the structure of community diversity influences precipitation-driven risk in multiple, and somewhat contrasting, ways.

Communities with low F_R and high MAT/MAP Risk are likely the most vulnerable to climate-driven changes in composition, as they face both, climate change–induced species turnover and a reduced capacity to maintain ecosystem function. These highly vulnerable sites are primarily located in the northern areas of the continent (Fig. 4). In contrast, communities with high F_R but high MAT/MAP Risk may still experience species loss but are expected to be more resilient in maintaining function; these are also concentrated in the continent's eastern interior. The least vulnerable communities—those with high F_R and low MAT/MAP Risk are scattered across central Australia (Fig. 4).

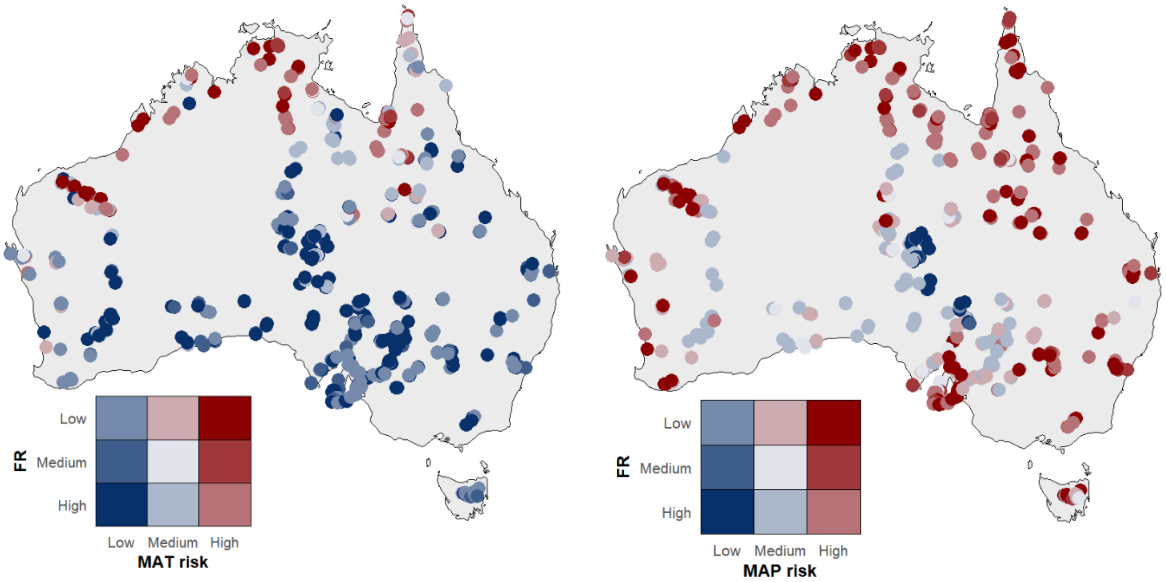

Figure 4. Bivariate maps of functional redundancy (F_R) and climate change risk across the Australian continent (646 TERN AusPlots). Left: F_R combined with mean annual temperature risk (MAT Risk). Right: F_R combined with mean annual precipitation risk (MAP Risk). For F_R, plots were categorized as low (bottom 33%), medium (33% up to the median of plots considered at risk), or high (above that median). For MAT Risk, plots with risk < 0 were classified as low risk, whereas for MAP Risk, plots with risk > 0 were classified as low risk. Plots at risk (MAT risk ≥ 0 or MAP risk ≤ 0), were split into medium and high risk categories using the median of the at-risk subset. Plots with high climate risk and low F_R (dark red) are potentially most vulnerable to climate-driven changes in community composition and associated loss of ecosystem functionality.

Table 2. Best-fit linear models explaining variation in MAT Risk and MAP Risk against bioclimatic predictors across Australia and within selected biomes. Models were selected using AIC-based stepwise selection. The table reports the retained predictors, model fit statistics (R^2, adjusted R^2, sigma), and information criteria (AIC, BIC). The direction and statistical significance of each predictor in the best model are shown in brackets after each term (+: positive effect; –: negative effect; * $p \leq 0.05$, ** $p \leq 0.01$, *** $p \leq 0.001$). Predictors without brackets were retained in the best model but were not statistically significant.

Response Variable	Best model formula	R^2	Adj R^2	sigma	AIC	BIC	$df_{residual}$
The whole Australia – All AusPlots							
MAT Risk	MAT Risk ~ 1 + MAT$^{(-*)}$ + T_Max$^{(+***)}$ + T_Range$^{(-***)}$ + P_Season$^{(+***)}$	0.712	0.710	1.292	2372.09	2399.45	701
MAP Risk	MAP Risk ~ 1 + MAT$^{(+***)}$ + T_Max$^{(-***)}$ + T_Range$^{(+***)}$ + MAP$^{(-***)}$ + P_Dry$^{(-*)}$	0.880	0.879	94.066	8427.64	8459.55	700
Biome 4 – Temperate broadleaf and mixed forests							
MAT Risk	MAT Risk ~ 1 + MAT$^{(+***)}$ + P_Dry	0.403	0.369	1.448	140.84	147.39	35
MAP Risk	MAP Risk ~ 1 + MAT$^{(-*)}$ + T_Max$^{(+*)}$ + T_Range$^{(-*)}$ + MAP$^{(+***)}$ + P_Dry$^{(-*)}$	0.750	0.711	144.866	493.47	504.93	32
Biome 7 – Tropical / subtropical grasslands, savannas and shrublands							
MAT Risk	MAT Risk ~ 1 + MAT$^{(+***)}$ + T_Range$^{(+***)}$ + P_Dry$^{(+***)}$	0.762	0.758	0.692	413.93	430.27	190
MAP Risk	MAP Risk ~ 1 + MAT + T_Max$^{(+***)}$ + T_Range$^{(-***)}$ + MAP$^{(+***)}$ + P_Season$^{(-***)}$	0.868	0.864	107.674	2373.95	2396.82	188
Biome 12 – Mediterranean forests, woodlands and shrublands							
MAT Risk	MAT Risk ~ 1 + T_Max$^{(+***)}$ + P_Season$^{(+***)}$	0.272	0.264	1.570	704.44	717.36	184
MAP Risk	MAP Risk ~ 1 + MAT$^{(+***)}$ + MAP$^{(+***)}$ + P_Season$^{(-***)}$	0.803	0.800	65.296	2099.56	2115.72	183
Biome 13 – Deserts and xeric shrublands							
MAT Risk	MAT Risk ~ 1 + MAT$^{(+***)}$ + T_Max$^{(+***)}$ + P-Dry$^{(-***)}$	0.770	0.767	0.940	673.78	691.31	242
MAP Risk	MAP Risk ~ 1 + MAT$^{(-***)}$ + T_Max$^{(+***)}$ + MAP$^{(+***)}$ + P-Dry$^{(+***)}$	0.858	0.856	36.140	2470.07	2491.10	241

Table 3. Best-fit linear models explaining variation in MAT Risk and MAP Risk against biodiversity metrics across Australia and within selected biomes. Models were selected using AIC-based stepwise selection. The table reports the retained predictors, model fit statistics (R^2, adjusted R^2, sigma), and information criteria (AIC, BIC). The direction and statistical significance of each predictor in the best model are shown in brackets after each term (+: positive effect; –: negative effect; * $p \leq 0.05$, ** $p \leq 0.01$, *** $p \leq 0.001$). Predictors without brackets were retained in the best model but were not statistically significant.

Response Variable	Best model formula	R^2	Adj R^2	sigma	AIC	BIC	$df_{residual}$
The whole Australia – All AusPlots							
MAT Risk	MAT Risk ~ 1	0.000	0.000	2.38	2954.80	2963.74	645
MAP Risk	MAP Risk ~ 1 + $S_R^{(-***)}$	0.169	0.168	236.82	8901.01	8914.42	644
Biome 4 – Temperate broadleaf and mixed forests							
MAT Risk	MAT Risk ~ 1 + S_R	0.083	0.052	1.854	134.24	138.64	30
MAP Risk	MAP Risk ~ 1 + $S_R^{(-***)}$	0.414	0.394	223.714	441.01	445.41	30
Biome 7 – Tropical / subtropical grasslands, savannas and shrublands							
MAT Risk	MAT Risk ~ 1	0.000	0.000	1.394	608.88	615.19	172
MAP Risk	MAP Risk ~ 1 + $S_R^{(+***)}$ + F_D	0.234	0.225	245.523	2400.10	2412.71	170
Biome 12 – Mediterranean forests, woodlands and shrublands							
MAT Risk	MAT Risk ~ 1 + $S_R^{(+**)}$	0.046	0.041	1.742	671.14	680.53	167
MAP Risk	MAP Risk ~ 1 + $S_R^{(+***)}$ + $F_R^{(-**)}$	0.232	0.223	129.872	2129.47	2141.99	166
Biome 13 – Deserts and xeric shrublands							
MAT Risk	MAT Risk ~ 1 + $S_D^{(-*)}$ + $F_D^{(+*)}$	0.030	0.022	1.912	972.41	986.23	231
MAP Risk	MAP Risk ~ 1 + $S_R^{(+***)}$ +$S_D^{(-***)}$ + $F_D^{(+***)}$	0.171	0.160	88.621	2768.72	2785.99	230

583 **4. Discussion**

584 Here, we analysed multiple diversity metrics —including species richness, species diversity,
585 functional diversity, and functional redundancy, but with particular emphasis on functional
586 redundancy (F_R)— in Australian plant communities using continental-scale ecological and
587 functional trait datasets. Our results showed that the northern and eastern Australian coastlines,
588 as well as Mediterranean-climate regions in southwestern Western Australia and southeastern
589 South Australia, are particularly vulnerable to species loss, shifts in community composition,
590 and subsequent loss of ecosystem function under climate change. We find F_R was generally
591 high across sampled communities, suggesting some resilience to loss of ecosystem function in
592 the event of species loss (Walker 1995; Pimiento *et al.* 2020). Central, arid plant communities
593 may be more resilient to functional loss in the event of species loss given the structured pattern
594 emerging of increasing F_R with distance from the coast. At the continental scale, F_R variation
595 was related to macroclimate in terms of both, temperature (MAT) and precipitation seasonality
596 patterns (positive and negative relationships, respectively), while S_R, S_D and F_D showed
597 opposite patterns (negative relationships with MAT and positive with MAP). However, these
598 relationships explained limited variance, likely because macroclimate metrics do not capture
599 fine-scale environmental variation, which can be a stronger driver of community composition.
600 Declines in S_R with increasing temperature range suggest thermal variability acts as a filter,
601 favouring stress-tolerant or generalist species, which could subsequently reduce F_D even if
602 overall abundance is maintained. F_R may buffer functional loss, but this is context-dependent
603 and often coincides with lower F_D, reflecting interactions between habitat filtering and niche
604 partitioning (Spasojevic and Suding 2012). These patterns underscore how functional traits and
605 climatic variability combined shaping ecosystem resilience, and emphasise the need to
606 understand how F_R and F_D respond to environmental gradients for conservation planning.

607 Andrew *et al.* (2021) found that F_D across Australian vegetation was strongly linked to
608 climate using grid-cell-based models. In contrast, our plot-based analyses suggest communities
609 may possess greater F_R than broad-scale patterns would indicate, as local assembly processes—
610 environmental filtering and biotic interactions—can enhance F_R, whereas grid-cell models
611 reflect broader niche–environment relationships. Similarly, Guerin *et al.* (2022) found strong
612 climate–trait links at the single-trait level across the same plot network, suggesting that
613 aggregating traits into composite F_D and F_R metrics may dilute finer-scale trait–environment
614 relationships. Although single trait studies can better reveal functional responses to
615 environmental gradients (e.g., Funk *et al.* 2017), reductionist approaches offer more limited
616 insights into community dynamics. Community assembly operates hierarchically, with

617 macroclimate dominating at large scales and local factors shaping communities locally (Diaz
618 et al. 1998; Laliberté et al. 2010). Consistent with this, we found that biome-scale relationships
619 between diversity metrics and climate were notably stronger than continental-scale patterns,
620 particularly in Mediterranean forests (biome 12) and tropical/subtropical grasslands (biome 7),
621 suggesting that smaller-scale analyses capture more coherent functional responses (Bruelheide
622 *et al.* 2018).

623 At the biome scale, diversity metrics responded to bioclimate in highly context-specific
624 ways, reflecting how climate interacts with physiology, resource availability, and evolutionary
625 history to shape plant communities. The contrasting responses of communities' F_R to
626 bioclimatic factors within biomes point to different drivers depending on the limiting factor or
627 stressor within each climate. In tropical savannas (biome 7), extreme rainfall seasonality limits
628 species with narrow niches, yet F_R increases with temperature range, likely reflecting
629 convergence on heat-adapted strategies. Temperate forests (biome 4), with more benign
630 climatic conditions, exhibit richness increase with warmth and species diversity increase with
631 rainfall, while F_R remains largely independent of climate, suggesting the absence of a strong
632 limiting stressor. Mediterranean systems (biome 12) experience dual pressures of intense heat
633 and summer drought, which reduce S_R and S_D under hotter conditions, yet F_R increases with
634 reduced precipitation, most likely through the prevalence of stress-avoidance traits. Deserts
635 (biome 13) show strong drought-driven F_R, although extreme heat constrains it. In line with
636 this, our results showed lower F_D at hotter and drier locations, and higher F_D at cooler and
637 wetter locations – supported by Guerin *et al.* (2022) who showed F_D declined with aridity,
638 pointing towards trait convergence with extreme conditions. These patterns indicate that F_D-
639 to-F_R ratio emerges from the interplay of habitat filtering, niche partitioning, and local
640 environmental constraints, producing contrasting functional responses across biomes rather
641 than reflecting climate alone. Consequently, communities with high F_D may have low F_R and
642 therefore be more vulnerable to species loss, whereas those with lower functionality may be
643 more resilient (Ricotta *et al.* 2016).

644 Short-term drivers such as land-use change, disease, and direct anthropogenic pressures
645 may further reduce F_R (Fonseca and Ganade 2001); however, our study focused on plant
646 communities with minimal recent disturbance, suggesting that higher F_R under extreme
647 environments reflects long-term environmental effects rather than human impact. We note,
648 however, that because our analyses rely on contemporary surveys, current species composition
649 may already incorporate recent climate- and land-use-driven shifts, which could influence trait
650 filtering patterns and reduce predictive power. Inconsistent F_R metrics also complicate

comparisons, emphasizing the need for clear methodology and fine-resolution environmental data when studying F_D and F_R (Biggs *et al.* 2020). Thus, we recommend clearly specifying F_R calculations and noting that functional similarity does not always imply redundancy, and we advocate for the use of finer-resolution environmental data (e.g., biome- or regional-scale) where available, to better elucidate F_D-to-F_R ratio and trends.

4.1. Climate change risk

Climate change risk exhibited clear geographic patterns across Australian plant communities and was strongly related to current climatic conditions, indicating that species safety margins may be more important than predicted exposure in determining the risk of species turnover or changes in community composition. Temperature-related risk (MAT Risk) varied with latitude, increasing from south to north (also supported by Gallagher *et al.* 2019), while precipitation-related risk (MAP Risk) was greatest in the coastline of the continent, especially in the North and in mediterranean-climate regions, and lowest at the arid centre. This, therefore, points to the northern coastline as a priority region for conservation practices to mitigate climate-driven change in vegetation communities.

In general, we found strong links between climate change risk and current climate conditions. The trends we found reflect the fact that as climates become more extreme in temperature, species approach their tolerance limits, leading to the greatest temperature-driven turnover in the hottest and most seasonally variable environments (Deutsch et al. 2008). For example, our findings that MAT Risk increased with long-term T-max and P-Season and decrease with MAT and T-Range, suggest that communities exposed to persistently high temperature extremes and strong intra-annual rainfall variability will be most sensitive to future warming, whereas broader thermal ranges may buffer against turnover. In contrast, MAP Risk was highest in sites that are warm and experience pronounced temperature fluctuations, but lowest in sites with high rainfall and dry-season precipitation, implying that plant communities subjected to the combination of heat and drought will experience higher precipitation-driven risk. Furthermore, this suggests that safety margins may be more important than exposure *per se* in determining sensitivity to climate change vulnerability in Australian plant communities (Foden et al. 2019), as the former takes a much wider range of values in Australian plant communities. We acknowledge that species' climate tolerances are derived from their realised rather than fundamental niches, potentially underestimating true physiological limits and adaptive capacity (Sax *et al.* 2013). Yet, species already persisting in extreme environments

seem to possess greater adaptive potential precisely because of being shaped by harsher conditions (Chevin and Hoffmann 2017).

Tropical savannas in northern Australia, where MAT Risk was found to be highest, are key global carbon sinks (Grace *et al.* 2006) that rely on complex interactions between fire regimes, water availability and vegetation dynamics (Moore *et al.* 2018), making them highly vulnerable to climatic shifts. Their high sensitivity to future precipitation shifts (MAP Risk) likely stem from the fact that these ecosystems are structured around strong wet–dry seasonality, where even small changes in rainfall amount or timing can disrupt plant recruitment, survival, and competitive ability. Unlike species in more southern arid zones, many northern taxa are less drought-adapted, thus, reduced rainfall could push them beyond their physiological limits. Moreover, biogeographic barriers constrain range shifts, as deserts to the south and oceans to the north limit gradual migration. Together, these factors indicate that northern Australia warrants particular attention from land managers and conservation purposes to prevent climate-driven species loss.

Mediterranean regions in the South West Australian Floristic Region (SWAFR) and South Australia showed high MAP Risk probably due to many species in these communities already nearing their upper climate thresholds, particularly with regards to the intense summer drought periods they face (Lewandrowski *et al.* 2021). In fact, drought-related dieback of Australian mediterranean vegetation has been well-documented, with rainfall already in decline and predicted to continue (Brouwers *et al.* 2013). Arid interiors exhibit low MAP Risk, due to projected increases in precipitation by 2070 (Gallagher *et al.* 2019). These biome-specific contrasts underscore the challenge of making generalizations when predicting changes in vegetation dynamics (Mori 2011).

At the biome scale, the links between climatic variables and MAT and MAP Risk highlight how different vegetation types may be exposed to shifts in community composition under warming and drying trends. The benign climatic conditions of temperate forests (biome 4) make them vulnerable to temperature stress (i.e. increases in MAT and T-Max positively affect MAT and MAP Risk respectively) and rainfall (i.e. lower P-Dry results in higher MAP Risk), reflecting their dependence on stable mild temperatures and moisture regimes. In tropical savannas (biome 7), MAT Risk increased in hotter sites and in areas with greater dry-season rainfall, indicating that both chronic warmth and large annual temperature fluctuations amplify sensitivity to warming. MAP Risk, by contrast, was highest in wetter and more heat-exposed savannas but declined with greater temperature range and rainfall seasonality, suggesting that climatic variability and pronounced wet–dry cycles may help buffer these

communities against precipitation-driven change. In Mediterranean systems (biome 12), both MAT and MAP Risk were highest in the warmest areas and in sites with weaker rainfall seasonality, indicating that communities occupying the margins of the Mediterranean climate regime—where summer drought is less pronounced—are more vulnerable to climate-driven change than those in strongly seasonal, drought-adapted environments, pointing to the importance of stress-tolerant adaptations in buffering these communities against increasing drought. In deserts (biome 13), MAT Risk was greatest in the hottest sites and declined with P-Dry, indicating that hyper-arid communities already adapted to extreme water limitation may be less sensitive to further warming than those in comparatively milder desert environments. MAP Risk, however, increased in warmer and wetter desert areas and in sites where the driest month is less dry, suggesting that communities located in more semi-arid areas are more vulnerable to precipitation-driven change than those in the most extremely water-limited regions that are already adapted to drought. Together, these contrasting biome-level responses indicate that climate-change risk is shaped not only by absolute climatic stress but by how far future conditions will diverge from the specific adaptive strategies of the vegetation characteristic of each biome, thus underscoring the need for case-by-case assessments. Although we focused on mean climate changes, we acknowledge that extreme events (e.g. heatwaves, droughts and wildfires) can also shape species survival and drive ecosystem shifts (Lloret *et al.* 2012).

4.2. Relationship between functional redundancy and climate change risk

By integrating climate change risk with F_R, we provide a robust assessment of Australian plant communities, capturing both their vulnerability to species loss and their potential resilience to functional disruption (traditionally ignored in climate change studies; Li *et al.* 2018). In this framework, communities with high climate risk and low F_R are most vulnerable, whereas those with high risk but high F_R may withstand some functional loss, and communities with low climate risk are inherently less threatened. At the continental-scale the negative relationship found between F_R and precipitation-driven climate change risk, points out to the north and east coastlines as well as the mediterranean-climate regions as the most vulnerable areas to suffer changes in community composition and subsequent loss of ecosystem function.

Unlike MAT Risk, MAP Risk exhibited clear relationships with community diversity metrics, reflecting the strong influence of rainfall and its seasonality on Australian plant communities. At the continental scale, communities with higher species richness experienced

lower MAP Risk, suggesting that richer communities are more buffered against precipitation-driven turnover.

At the biome scale, the influence of community diversity on climate-change risk varied markedly. In temperate forests (biome 4), higher species richness appeared to buffer communities against precipitation-driven turnover, suggesting that diverse forests maintain stability under altered rainfall regimes. In tropical savannas (biome 7), communities with larger species pools seem to be subjected to amplified compositional shifts under warming and altered rainfall, perhaps reflecting the exposure of less stress-tolerant species in these dynamic environments. In Mediterranean systems (biome 12) functional redundancy plays a key role, mitigating precipitation-driven risk, and highlighting the role of overlapping functional traits in stabilizing communities despite turnover in species composition. In deserts (biome 13), the contrasting effects of species and functional diversity climate-driven risk suggest that the vulnerability of arid communities is shaped by the balance between the breadth of functional strategies and species identities, with some aspects of diversity enhancing turnover while others confer resilience. Altogether, these patterns indicate that precipitation-driven climate risk is in general more sensitive to community structure than temperature-driven risk, and that the ecological consequences of diversity for climate vulnerability are highly context-dependent, reflecting the specific adaptive strategies and functional composition of each biome.

The concept of functional redundancy deals with the local extinction of species, yet climate change may also add novel species, which can have diverse functional effects—from enhancing community resilience supporting mutualistic interactions, as seen on islands (Traveset *et al.* 2013), to detrimental impacts from non-native species (Wardle *et al.* 2011). Accounting for both, species gain and loss, is therefore essential to accurately predict climate-driven community responses (Gallagher *et al.* 2013). A limitation of using F_R to estimate community resilience is that a set of functionally redundant species can theoretically all respond similarly to a given threat, resulting in loss of ecosystem function (Mori *et al.* 2013). Thus, community resilience depends on both response diversity—the variety of species' functional response traits—and functional redundancy (Elmqvist *et al.* 2003; Mori *et al.* 2013). Ideally, F_R would be measured using effect traits with explicit links to a given ecosystem function and response traits with explicit links to a given threat; however, this is difficult as traits can often act as either depending on context (Suding *et al.* 2008). Additionally, at the continental-scale trait data availability is in general limited, reinforcing the importance of large open access trait databases such as AusTraits (Falster *et al.* 2021) and the ongoing work by numerous researchers to improve the taxonomic coverage of trait data. Because of the present

barriers to implementing the effect- response framework, the assumption that a higher degree of functional redundancy infers at least some degree of response diversity is often made (Laliberté *et al.* 2010; Pillar *et al.* 2013).

While we retain the term "functional redundancy" for comparability with previous studies, we frame F_R as functional similarity—a spectrum of overlapping but non-identical contributions to ecosystem processes—acknowledging concerns that the term redundancy may be ecologically misleading or counterproductive (Eisenhäuser *et al.* 2023). While Fischer and de Bello (2003) suggested redundancy implied resilience, with the loss of some species having little detectable effect at the community scale, Eisenhäuser *et al.* (2023) argue this framing risks underestimating the unique and context-dependent contributions of species to ecosystem functioning. We agree that the term "redundancy" can obscure the fact that species' roles are not interchangeable across space, time, or environmental conditions; thus, F_R should be interpreted here as functional similarity—recognizing that resilience is not guaranteed and functional loss might still remain a risk.

Our findings can be useful to land managers and policy makers and guide conservation prioritization (Walker 1995; Rosenfeld 2002) in Australia, especially in highly vulnerable areas like the tropical North and the Mediterranean regions. Deliberately preserving high-F_R communities could also help maintaining key ecosystem functionality (Mori *et al.* 2013). Having established F_R and climate-driven risk across plant communities in the Australian continent, future work should explicitly test whether F_R effectively enhances resilience over time—a crucial step given limited knowledge under certain conditions (Biggs et al. 2020).

4.3. Future directions

Future research should test whether functional redundancy enhances ecosystem resilience over time, leveraging networks such as TERN AusPlots to track changes in functional diversity and ecosystem function before and after disturbances. Remote sensing (e.g., NDVI) could complement plot data for retrospective analyses, enabling assessment of productivity responses to environmental stressors such as drought. For example, Aguirre-Gutiérrez et al. (2022) linked aboveground biomass stability to F_R in tropical forest plots following an El Niño drying event. While assisted translocation of functionally rare species may be required in extreme cases, a pragmatic approach emphasizes monitoring, maintaining habitat quality, supporting natural regeneration, and mitigating pressures such as altered fire regimes or invasive species. This strategy allows management without assuming that redundancy guarantees resilience, while keeping interventions open when critical functions are at risk. Long-term, standardized

monitoring combined with trait-based analyses is therefore essential, and the integration of AusPlots and AusTraits provides a robust foundation to couple F_R with climate risk, identify conservation priorities, and anticipate when ecosystem resilience may be compromised.

5. Conclusions

Australian plant communities show strong regional variation in vulnerability to climate change, with the tropical north being at greatest risk due to shifts in rainfall and temperature combined with low functional redundancy, followed by the mediterranean regions of Western and South Australia. Communities with high climate risk and low redundancy are particularly prone to losing functionally unique species, thereby threatening ecosystem stability. These findings highlight priority areas for monitoring and management, providing a framework to safeguard ecosystem function under a changing climate. Targeted monitoring and prioritizing proactive management in these hotspots of high at-risk vegetation communities is therefore critical to prevent irreversible functional loss under future climate scenarios.

Author Contributions

I.M.-F. and G.R.G. had the initial idea for the paper. R.V.M., I.M.-F., and S.C.A. contributed to data analysis; I.M.-F. and R.V.M. produced results and figures with recommendations from other authors. All authors contributed to drafting the paper, reviewed the manuscript and gave final approval for publication.

Acknowledgements

The AusTraits project received investment (https://doi.org/10.47486/TD044, https://doi.org/10.47486/DP720) from the Australian Research Data Commons (ARDC). The ARDC is funded by the National Collaborative Research Infrastructure Strategy (NCRIS). This work is supported by the use of Terrestrial Ecosystem Research Network (TERN) infrastructure, which is enabled by the Australian Government's National Collaborative Research Infrastructure Strategy (NCRIS).

References

Ackerly, DD, Cornwell, WK (2007) A trait-based approach to community assembly: partitioning of species trait values into within-and among-community components. *Ecology Letters* **10**, 135-145.

Aguirre-Gutiérrez, J, Berenguer, E, Oliveras Menor, I, Bauman, D, Corral-Rivas, JJ, Nava-Miranda, MG, Both, S, Ndong, JE, Ondo, FE, Bengone, NNs, Mihinhou, V, Dalling, JW, Heineman, K, Figueiredo, A, González-M, R, Norden, N, Hurtado-M, AB, González, D, Salgado-Negret, B, Reis, SM, Moraes de Seixas, MM, Farfan-Rios, W, Shenkin, A, Riutta, T, Girardin, CAJ, Moore, S, Abernethy, K, Asner, GP, Bentley, LP, Burslem, DFRP, Cernusak, LA, Enquist, BJ, Ewers, RM, Ferreira, J, Jeffery, KJ, Joly, CA, Marimon-Junior, BH, Martin, RE, Morandi, PS, Phillips, OL, Bennett, AC, Lewis, SL, Quesada, CA, Marimon, BS, Kissling, WD, Silman, M, Teh, YA, White, LJT, Salinas, N, Coomes, DA, Barlow, J, Adu-Bredu, S, Malhi, Y (2022) Functional susceptibility of tropical forests to climate change. *Nature Ecology & Evolution* **6**, 878-889.

Andrew, SC, Mokany, K, Falster, DS, Wenk, E, Wright, IJ, Merow, C, Adams, V, Gallagher, RV (2021) Functional diversity of the Australian flora: strong links to species richness and climate. *Journal of Vegetation Science* **32**, e13018.

Andrew, SC, Martín-Forés, I, Guerin, G, Coleman, D, Falster, D, Wenk, E, Wright, I, Gallagher, RV (2025). Mapping plant functional traits using gap-filled datasets to inform management and modelling. Global Ecology and Biogeography.

Aphalo P (2025). _ggpmisc: Miscellaneous Extensions to 'ggplot2'_.

Bailey, HP (1964). Toward a unified concept of the temperate climate. *Geographical Review*, **54**, 516-545.

Bates, DM, 2010. lme4: Mixed-effects modeling with R. Springer New York,

Bennett, JM, Sunday, J, Calosi, P, Villalobos, F, Martínez, B, Molina-Venegas, R, ..., Olalla-Tárraga, MÁ (2021) The evolution of critical thermal limits of life on Earth. *Nature communications*, **12**, 1198.

Biggs, CR, Yeager, LA, Bolser, DG, Bonsell, C, Dichiera, AM, Hou, Z, Keyser, SR, Khursigara, AJ, Lu, K, Muth, AF (2020) Does functional redundancy affect ecological stability and resilience? A review and meta-analysis. *Ecosphere* **11**, e03184.

Borgy, B, Violle, C, Choler, P, Garnier, E, Kattge, J, Loranger, J, Amiaud, B, Cellier, P, Debarros, G, Denelle, P (2017) Sensitivity of community-level trait–environment relationships to data representativeness: A test for functional biogeography. *Global Ecology and Biogeography* **26**, 729-739.

Botta-Dukát, Z (2005) Rao's quadratic entropy as a measure of functional diversity based on multiple traits. *Journal of Vegetation Science* **16**, 533-540.

Brouwers, NC, Mercer, J, Lyons, T, Poot, P, Veneklaas, E, Hardy, G (2013) Climate and landscape drivers of tree decline in a Mediterranean ecoregion. *Ecology and Evolution* **3**, 67-79.

Bruelheide, H, Dengler, J, Purschke, O, Lenoir, J, Jiménez-Alfaro, B, Hennekens, SM, Botta-Dukát, Z, Chytrý, M, Field, R, Jansen, F, Kattge, J, Pillar, VD, Schrodt, F, Mahecha, MD, Peet, RK, Sandel, B, van Bodegom, P, Altman, J, Alvarez-Dávila, E, Arfin Khan, MAS, Attorre, F, Aubin, I, Baraloto, C, Barroso, JG, Bauters, M, Bergmeier, E, Biurrun, I, Bjorkman, AD, Blonder, B, Čarni, A, Cayuela, L, Černý, T, Cornelissen, JHC, Craven, D, Dainese, M, Derroire, G, De Sanctis, M, Díaz, S, Doležal, J, Farfan-Rios, W, Feldpausch, TR, Fenton, NJ, Garnier, E, Guerin, GR, Gutiérrez, AG, Haider, S, Hattab, T, Henry, G, Hérault, B, Higuchi, P, Hölzel, N, Homeier, J, Jentsch, A, Jürgens, N, Kącki, Z, Karger, DN, Kessler, M, Kleyer, M, Knollová, I, Korolyuk, AY, Kühn, I, Laughlin, DC, Lens, F, Loos, J, Louault, F, Lyubenova, MI, Malhi, Y, Marcenò, C, Mencuccini, M, Müller, JV, Munzinger, J, Myers-Smith, IH, Neill, DA, Niinemets, Ü, Orwin, KH, Ozinga, WA, Penuelas, J, Pérez-Haase, A, Petřík, P, Phillips, OL, Pärtel, M, Reich, PB, Römermann, C, Rodrigues, AV, Sabatini, FM, Sardans, J, Schmidt, M, Seidler, G, Silva Espejo, JE, Silveira, M, Smyth, A, Sporbert, M, Svenning, J-C, Tang, Z, Thomas, R, Tsiripidis, I, Vassilev, K, Violle, C, Virtanen, R, Weiher, E*et al.* (2018) Global trait–environment relationships of plant communities. *Nature Ecology & Evolution* **2**, 1906-1917.

Cadotte, MW, Carscadden, K, Mirotchnick, N (2011) Beyond species: functional diversity and the maintenance of ecological processes and services. *Journal of applied ecology* **48**, 1079-1087.

Chevin, LM, Hoffmann, AA (2017) Evolution of phenotypic plasticity in extreme environments. *Philosophical Transactions of the Royal Society B: Biological Sciences* **372**, 20160138.

912 Deutsch, CA, Tewksbury, JJ, Huey, RB, Sheldon, KS, Ghalambor, CK, Haak, DC, Martin,
913 PR (2008) Impacts of climate warming on terrestrial ectotherms across latitude.
914 *Proceedings of the National Academy of Sciences* **105**, 6668-6672.
915 Díaz, S, Kattge, J, Cornelissen, JH, Wright, IJ, Lavorel, S, Dray, S, Reu, B, Kleyer, M, Wirth,
916 C, Colin Prentice, I (2016) The global spectrum of plant form and function. *Nature*
917 **529**, 167-171.
918 Díaz, S, Settele, J, Brondízio ES, Ngo, HT, Guèze, M, Agard, J, Arneth, A, Balvanera, P,
919 Brauman, KA, Butchart, SHM, Chan, KMA, Garibaldi, LA, Ichii, K, Liu, J,
920 Subramanian, SM, Midgley, GF, Miloslavich, P, Molnár, Z, Obura, D, Pfaff, A,
921 Polasky, S, Purvis, A, Razzaque, J, Reyers, B, Roy Chowdhury, R, Shin, YJ,
922 Visseren-Hamakers, IJ, Willis, KJ, Zayas, CN (Eds.). IPBES (2019): Summary for
923 policymakers of the global assessment report on biodiversity and ecosystem services
924 of the Intergovernmental Science-Policy Platform on Biodiversity and Ecosystem
925 Services. IPBES secretariat, Bonn, Germany. 56 pages.
926 Elmqvist, T, Folke, C, Nyström, M, Peterson, G, Bengtsson, J, Walker, B, Norberg, J (2003)
927 Response diversity, ecosystem change, and resilience. *Frontiers in Ecology and the*
928 *Environment* **1**, 488-494.
929 Eisenhäuer, N, Hines, J, Maestre, FT, Rillig, MC (2023). Reconsidering functional
930 redundancy in biodiversity research. npj Biodiversity, 2(1), 9.
931 Falster, D. S., & Westoby, M. (2003). Plant height and evolutionary games. *Trends in*
932 *Ecology & Evolution*, **18**, 337-343.
933 Falster, D, Gallagher, R, Wenk, EH, Wright, IJ, Indiarto, D, Andrew, SC, Baxter, C, Lawson,
934 J, Allen, S, Fuchs, A (2021) AusTraits, a curated plant trait database for the
935 Australian flora. *Scientific data* **8**, 1-20.
936 Fick, SE, Hijmans, RJ (2017) WorldClim 2: new 1-km spatial resolution climate surfaces for
937 global land areas. *International journal of climatology* **37**, 4302-4315.Fischer, FM, de
938 Bello, F (2023). On the uniqueness of functional redundancy. npj Biodiversity, 2(1),
939 23.
940 Foden, WB, Young, BE, Akçakaya, HR, Garcia, RA, Hoffmann, AA, Stein, BA, Thomas,
941 CD, Wheatley, CJ, Bickford, D, Carr, JA, Hole, DG, Martin, TG, Pacifici, M, Pearce-
942 Higgins, JW, Platts, PJ, Visconti, P, Watson, JEM, Huntley, B. (2019). Climate
943 change vulnerability assessment of species. Wiley interdisciplinary reviews: climate
944 change, 10(1), e551.

945 Fonseca, CR, Ganade, G (2001) Species functional redundancy, random extinctions and the
946 stability of ecosystems. *Journal of Ecology* 118-125.
947 Funk, JL, Larson, JE, Ames, GM, Butterfield, BJ, Cavender-Bares, J, Firn, J, Laughlin, DC,
948 Sutton-Grier, AE, Williams, L, Wright, J (2017) Revisiting the H oly G rail: using
949 plant functional traits to understand ecological processes. *Biological reviews* **92**,
950 1156-1173.
951 Gallagher, RV, Allen, S, Wright, IJ (2019) Safety margins and adaptive capacity of
952 vegetation to climate change. *Scientific Reports* **9**, 1-11.
953 Gallagher, RV, Hughes, L, Leishman, MR (2013) Species loss and gain in communities
954 under future climate change: consequences for functional diversity. *Ecography* **36**,
955 531-540.
956 Gallagher, RV, Falster, DS, Maitner, BS, Salguero-Gómez, R, Vandvik, V, Pearse, WD, ... &
957 Enquist, BJ (2020). Open Science principles for accelerating trait-based science
958 across the Tree of Life. Nature ecology & evolution, 4(3), 294-303.
959 Grace, J, José, JS, Meir, P, Miranda, HS, Montes, RA (2006) Productivity and carbon fluxes
960 of tropical savannas. *Journal of Biogeography* **33**, 387-400.
961 Guerin, GR, Gallagher, RV, Wright, IJ, Andrew, SC, Falster, DS, Wenk, E, Munroe, SEM,
962 Lowe, AJ, Sparrow, B (2022) Environmental associations of abundance-weighted
963 functional traits in Australian plant communities. *Basic and Applied Ecology* **58**, 98-
964 109.
965 Guerin, GR, Williams, KJ, Sparrow, B, Lowe, AJ (2020a) Stocktaking the environmental
966 coverage of a continental ecosystem observation network. *Ecosphere* **11**, e03307.
967 Guerin, G, Saleeba, T, Munroe, S, Blanco-Martin, B, Martín-Forés, I, Tokmakoff, A (2020b)
968 ausplotsR: TERN AusPlots analysis package. *R package version* **1**,Hooper, DU,
969 Adair, EC, Cardinale, BJ, Byrnes, JEK, Hungate, BA, Matulich, KL, Gonzalez, A,
970 Duffy, JE, Gamfeldt, L, O'Connor, MI (2012) A global synthesis reveals biodiversity
971 loss as a major driver of ecosystem change. *Nature* **486**, 105-108.
972 Hughes, L (2003) Climate change and Australia: trends, projections and impacts. *Austral*
973 *Ecology* **28**, 423-443.
974 Keith, DA (Ed.). (2017). Australian vegetation. Cambridge University Press.
975 Laliberté E, Wells, JA, DeClerck, F, Metcalfe, DJ, Catterall, CP, Queiroz, C, Aubin, I,
976 Bonser, SP, Ding, Y, Fraterrigo, JM (2010) Land-use intensification reduces
977 functional redundancy and response diversity in plant communities. *Ecology Letters*
978 **13**, 76-86.

Lancaster, LT, Humphreys, AM (2020) Global variation in the thermal tolerances of plants. *Proceedings of the National Academy of Sciences*, **117**, 13580-13587.

Lewandrowski, W, Stevens, JC, Webber, BL, L. Dalziell, E, Trudgen, MS, Bateman, AM, Erickson, TE (2021) Global change impacts on arid zone ecosystems: Seedling establishment processes are threatened by temperature and water stress. *Ecology and Evolution* **11**, 8071-8084.

Li, D, Wu, S, Liu, L, Zhang, Y, Li, S (2018) Vulnerability of the global terrestrial ecosystems to climate change. *Global change biology* **24**, 4095-4106.

Lionello, P, Malanotte-Rizzoli, P, Boscolo, R, Alpert, P, Artale, V, Li, L, ..., Xoplaki, E (2006). The Mediterranean climate: an overview of the main characteristics and issues. *Developments in Earth and Environmental Sciences*, **4**, 1-26.

Lloret, F, Escudero, A, Iriondo, JM, Martínez-Vilalta, J, Valladares, F (2012) Extreme climatic events and vegetation: the role of stabilizing processes. *Global change biology* **18**, 797-805.

Moore, CE, Beringer, J, Donohue, RJ, Evans, B, Exbrayat, J-F, Hutley, LB, Tapper, NJ (2018) Seasonal, interannual and decadal drivers of tree and grass productivity in an Australian tropical savanna. *Global change biology* **24**, 2530-2544.

Mori, AS (2011) Ecosystem management based on natural disturbances: hierarchical context and non-equilibrium paradigm. *Journal of applied ecology* **48**, 280-292.

Mori, AS, Furukawa, T, Sasaki, T (2013) Response diversity determines the resilience of ecosystems to environmental change. *Biological reviews* **88**, 349-364.

Munroe, S, Guerin, G, Saleeba, T, Martín-Forés, I, Blanco-Martin, B, Sparrow, B, Tokmakoff, A, 2021. ausplotsR: An R package for rapid extraction and analysis of vegetation and soil data collected by Australia's Terrestrial Ecosystem Research Network. Wiley Online Library,

Noy-Meir, I (1973). Desert ecosystems: environment and producers. *Annual review of ecology and systematics*, 25-51.

Olson, DM, Dinerstein, E, Wikramanayake, ED, Burgess, ND, Powell, GVN, Underwood, EC, D'amico, JA, Itoua, I, Strand, HE, Morrison, JC, Loucks, CJ, Allnutt, TF, Ricketts, TH, Kura, Y, Lamoreux, JF, Wettengel, WW, Hedao, P, Kassem, KR (2001) Terrestrial Ecoregions of the World: A New Map of Life on Earth: A new global map of terrestrial ecoregions provides an innovative tool for conserving biodiversity. *BioScience* **51**, 933-938.

Pettorelli, N, Graham, NA, Seddon, N, Maria da Cunha Bustamante, M, Lowton, MJ, Sutherland, WJ, ... & Barlow, J (2021) Time to integrate global climate change and biodiversity science-policy agendas. *Journal of Applied Ecology* **58**, 2384-2393.

Pillar, VD, Blanco, CC, Müller, SC, Sosinski, EE, Joner, F, Duarte, LD (2013) Functional redundancy and stability in plant communities. *Journal of Vegetation Science* **24**, 963-974.

Pimiento, C, Bacon, CD, Silvestro, D, Hendy, A, Jaramillo, C, Zizka, A, Meyer, X, Antonelli, A (2020) Selective extinction against redundant species buffers functional diversity. *Proceedings of the Royal Society B* **287**, 20201162.

RCoreTeam (2018) The R Stats Package *CRAN Repository, R*

Ricotta, C, de Bello, F, Moretti, M, Caccianiga, M, Cerabolini, BE, Pavoine, S (2016) Measuring the functional redundancy of biological communities: a quantitative guide *Methods in Ecology and Evolution* **7**, 1386-1395

Rosenfeld, JS (2002) Functional redundancy in ecology and conservation. *Oikos* **98**, 156-162.

Sax, DF, Early, R, Bellemare, J (2013) Niche syndromes, species extinction risks, and management under climate change. *Trends in ecology & evolution* **28**, 517-523.

Schrodt, F., Kattge, J., Shan, H., Fazayeli, F., Joswig, J., Banerjee, A., ... & Reich, P. B. (2015). BHPMF–a hierarchical Bayesian approach to gap-filling and trait prediction for macroecology and functional biogeography. *Global Ecology and Biogeography*, **24**, 1510-1521.

Shaw, RB, Jacobs, SWL, Everett, J (2000) Tropical grasslands and savannas. Grasses: Systematics and Evolution. CSIRO, Melbourne: CSIRO, 351-355.

Sparrow, BD, Foulkes, JN, Wardle, GM, Leitch, EJ, Caddy-Retalic, S, Van Leeuwen, SJ, Tokmakoff, A, Thurgate, NY, Guerin, GR, Lowe, AJ (2020) A vegetation and soil survey method for surveillance monitoring of rangeland environments. *Frontiers in Ecology and Evolution* **8**, 157.

Spasojevic, MJ, Suding, KN (2012) Inferring community assembly mechanisms from functional diversity patterns: the importance of multiple assembly processes. *Journal of Ecology* **100**, 652-661.

State of the Climate 2024, CSIRO and Bureau of Meteorology, © Government of Australia.

Suding, KN, Lavorel, S, Chapin Iii, F, Cornelissen, JH, Díaz, S, Garnier, E, Goldberg, D, Hooper, DU, Jackson, ST, Navas, ML (2008) Scaling environmental change through the community-level: A trait-based response-and-effect framework for plants. *Global change biology* **14**, 1125-1140.

Traveset, A, Heleno, R, Chamorro, S, Vargas, P, McMullen, CK, Castro-Urgal, R, Nogales, M, Herrera, HW, Olesen, JM (2013) Invaders of pollination networks in the Galápagos Islands: emergence of novel communities. *Proceedings of the Royal Society B: Biological Sciences* **280**, 20123040.

Valladares, F, Magro, S, Martín-Forés, I (2019). Anthropocene, the challenge for" Homo sapiens" to set its own limits. Cuadernos de Investigación Geográfica, 45(1), 33-59.

Violle, C, Reich, PB, Pacala, SW, Enquist, BJ, Kattge, J (2014) The emergence and promise of functional biogeography. *Proceedings of the National Academy of Sciences* **111**, 13690-13696.

Walker, B (1992) Biodiversity and ecological redundancy. *Conservation Biology*, **6**, 18–23.

Walker, B (1995) Conserving biological diversity through ecosystem resilience. *Conservation Biology* **9**, 747-752.

Wardle, DA, Bardgett, RD, Callaway, RM, Van der Putten, WH (2011) Terrestrial ecosystem responses to species gains and losses. *science* **332**, 1273-1277.

Westoby, M (1998) A leaf-height-seed (LHS) plant ecology strategy scheme. *Plant and soil* **199**, 213-227.

White, A, Sparrow, B, Leitch, E, Foulkes, J, Flitton, R, Lowe, AJ, Caddy-Retalic, S (2012) AUSPLOTS rangelands survey protocols manual.

Wickham, H. (2016) ggplot2: Elegant Graphics for Data Analysis. Springer-Verlag New York.

Wright, IJ, Reich, PB, Westoby, M, Ackerly, DD, Baruch, Z, Bongers, F, Cavender-Bares, J, Chapin, T, Cornelissen, JH, Diemer, M (2004) The worldwide leaf economics spectrum. *Nature* **428**, 821-827.

Supplementary material

Supplemental table S1. Pairwise comparisons of functional redundancy (F_R) among four Australian biomes (IDs Tropical/subtropical grasslands, savannas and shrublands = 4, Temperate broadleaf and mixed forests = 7, Mediterranean forests, woodlands and shrublands = 12, Deserts and xeric shrublands = 13) using Tukey's Honestly Significant Difference (HSD) test. The table shows the mean difference in F_R between each pair of biomes, the lower and upper bounds of the 95% confidence interval, and the adjusted p-value (Adjusted P-value) for multiple comparisons. Positive difference values indicate that the first biome listed in the comparison has higher F_R than the second.

Biome comparison	Difference	Lower_95CI	Upper_95CI	Adjusted P-value
7 vs. 4	0.043	0.008	0.079	≤0.01
12 vs. 4	0.017	-0.019	0.052	n.s.
13 vs. 4	0.050	0.015	0.084	≤0.01
12 vs. 7	-0.027	-0.046	-0.007	≤0.01
13 vs. 7	0.006	-0.012	0.025	n.s.
12 vs. 13	0.033	0.015	0.052	≤0.001

Supplemental table S2. Pearson correlation coefficients between pairs of climate variables. Values are shown for the upper triangle of the correlation matrix. Asterisks indicate significance levels: $p \leq 0.05$ (*), $p \leq 0.01$ (**), $p \leq 0.001$ (***).

	MAT	T-Range	T-Max	MAP	P-Dry	P-Seasonality
MAT	1	0.18***	0.87***	0.05	-0.83***	0.76***
T-Range		1	0.63***	-0.78***	-0.25***	-0.32***
T-Max			1	-0.37***	-0.8***	0.41***
MAP				1	0.3***	0.48***
P-Dry					1	-0.55***
P-Seasonality						1

Supplemental table S3. Pearson correlation coefficients between pairs of diversity metrics. Values are shown for the upper triangle of the correlation matrix. Asterisks indicate significance levels: $p \leq 0.05$ (*), $p \leq 0.01$ (**), $p \leq 0.001$ (***).

	Species richness (SR)	Species diversity (SD)	Functional diversity (FD)	Functional redundancy (FR)
Species richness (SR)	1	0.6***	0.52***	-0.13**
Species diversity (SD)		1	0.67***	0.06
Functional diversity (FD)			1	-0.69***
Functional redundancy (FR)				1

Supplemental table S4. Coefficients from the best-supported linear regression models for plant diversity metrics (S_R, S_D, F_D, F_R) against bioclimatic variables at continental and biome scales. Shown are the estimated slope (estimate), standard error (std.error), t-value (statistic), and p-value for each predictor in the model. Models were selected based on the lowest AIC, and only the best-supported models are presented.

Scale	Response	term	estimate	std.error	statistic	p.value
Continental	S_R	(Intercept)	24.2378	5.3295	4.5479	0.0000
		MAT	-2.4493	0.5898	-4.1529	0.0000
		T_Max	2.2499	0.6237	3.6076	0.0003
		T_Range	-1.3610	0.3007	-4.5261	0.0000
		MAP	0.0090	0.0018	4.9067	0.0000
		P_Season	0.0515	0.0261	1.9722	0.0490
	S_D	(Intercept)	0.9812	0.0698	14.0517	0.0000
		MAT	-0.0138	0.0031	-4.5262	0.0000
		MAP	0.0002	0.0000	6.7622	0.0000
		P_Dry	-0.0041	0.0011	-3.5507	0.0004
	F_D	(Intercept)	0.2397	0.0385	6.2291	0.0000
		MAT	-0.0132	0.0031	-4.2162	0.0000
		T_Max	0.0090	0.0040	2.2219	0.0266
		T_Range	-0.0041	0.0024	-1.7305	0.0840
		MAP	0.0001	0.0000	3.7973	0.0002
		P_Dry	-0.0015	0.0006	-2.6001	0.0095
	F_R	(Intercept)	0.7850	0.0391	20.0707	0.0000
		MAT	0.0165	0.0043	3.8009	0.0002
		T_Max	-0.0145	0.0046	-3.1631	0.0016
		T_Range	0.0058	0.0022	2.6490	0.0083
		MAP	0.0000	0.0000	-1.5771	0.1153
		P_Season	-0.0004	0.0002	-2.2628	0.0240
Biome 4	S_R	(Intercept)	71.1624	13.6375	5.2181	0.0000
		T_Max	3.5419	0.5766	6.1431	0.0000
		T_Range	-5.8727	1.0443	-5.6235	0.0000
	S_D	(Intercept)	0.6769	0.2134	3.1717	0.0038
		MAT	0.0160	0.0104	1.5366	0.1360
		MAP	0.0012	0.0004	3.4262	0.0020
		P_Dry	-0.0155	0.0064	-2.4373	0.0217
		P_Season	-0.0213	0.0077	-2.7533	0.0104
	F_D	(Intercept)	0.4416	0.0925	4.7714	0.0000
		T_Range	-0.0106	0.0043	-2.4727	0.0193
	F_R	(Intercept)	0.6680	0.0393	16.9800	0.0000
		MAT	0.0041	0.0030	1.3494	0.1873
Biome 7	S_R	(Intercept)	116.8951	23.9447	4.8819	0.0000
		MAT	4.5659	0.7575	6.0276	0.0000
		T_Max	-4.5345	0.5650	-8.0260	0.0000
		P_Dry	-0.7088	0.2469	-2.8706	0.0046
		P_Season	-0.4184	0.0858	-4.8774	0.0000

	S_D	(Intercept)	0.4751	0.1772	2.6813	0.0081
		MAT	0.0151	0.0105	1.4436	0.1507
		MAP	0.0002	0.0000	4.6174	0.0000
		P_Season	-0.0026	0.0011	-2.3385	0.0205
	F_D	(Intercept)	0.1647	0.0207	7.9457	0.0000
		MAP	0.0001	0.0000	5.3350	0.0000
		P_Season	-0.0004	0.0002	-2.0817	0.0389
	F_R	(Intercept)	0.6914	0.0285	24.2331	0.0000
		T_Range	0.0029	0.0011	2.4919	0.0137
Biome 12	S_R	(Intercept)	38.3001	11.2007	3.4195	0.0008
		MAT	-4.6103	0.8921	-5.1679	0.0000
		T_Max	1.4021	0.4222	3.3212	0.0011
		P_Dry	0.4095	0.1826	2.2428	0.0263
		P_Season	0.4118	0.0468	8.8063	0.0000
	S_D	(Intercept)	1.0220	0.1279	7.9920	0.0000
		MAT	-0.0214	0.0071	-3.0246	0.0029
		P_Season	0.0026	0.0006	4.4678	0.0000
	F_D	(Intercept)	0.0664	0.0212	3.1279	0.0021
		P_Dry	0.0048	0.0010	4.7827	0.0000
		P_Season	0.0016	0.0003	6.4811	0.0000
	F_R	(Intercept)	1.2241	0.0946	12.9357	0.0000
		MAT	-0.0201	0.0045	-4.4583	0.0000
		MAP	-0.0002	0.0000	-5.0010	0.0000
		P_Dry	-0.0044	0.0011	-3.9035	0.0001
Biome 13	S_R	(Intercept)	-3.5374	11.1735	-0.3166	0.7518
		MAT	-3.3824	0.9721	-3.4794	0.0006
		T_Max	3.2492	1.1072	2.9346	0.0037
		T_Range	-1.1241	0.5525	-2.0346	0.0430
		MAP	0.0409	0.0085	4.8065	0.0000
	S_D	(Intercept)	0.7469	0.0237	31.5031	0.0000
		P_Season	-0.0009	0.0004	-2.1098	0.0359
	F_D	(Intercept)	0.0770	0.0921	0.8360	0.4040
		MAT	-0.0271	0.0072	-3.7806	0.0002
		T_Max	0.0161	0.0045	3.6048	0.0004
		MAP	0.0001	0.0001	1.5899	0.1132
		P_Season	0.0011	0.0005	2.4453	0.0152
	F_R	(Intercept)	0.8491	0.0940	9.0303	0.0000
		MAT	0.0177	0.0051	3.4729	0.0006
		T_Range	-0.0113	0.0024	-4.6601	0.0000
		MAP	-0.0002	0.0001	-2.3200	0.0212
		P_Season	-0.0015	0.0005	-3.0192	0.0028

Supplemental table S5. Coefficients from the best-supported linear regression models for climate-driven risk (MAT Risk and MAP Risk) against bioclimatic variables at continental and biome scales. Shown are the estimated slope (estimate), standard error (std.error), t-value (statistic), and p-value for each predictor in the model. Models were selected based on the lowest AIC, and only the best-supported models are presented.

Scale	Response	Term	Estimate	Std error	Statistic	P-value
Continental	risk_MAT	(Intercept)	-11.37	0.46	-24.81	0.0000
		MAT	-0.16	0.07	-2.16	0.0315
		P_Season	0.03	0.00	10.31	0.0000
		T_Max	0.45	0.08	5.83	0.0000
		T_Range	-0.16	0.04	-4.25	0.0000
	risk_MAP	(Intercept)	480.92	56.07	8.58	0.0000
		MAP	-0.63	0.02	-25.31	0.0000
		MAT	20.29	4.57	4.44	0.0000
		P_Dry	-2.08	0.84	-2.47	0.0139
		T_Max	-39.47	5.89	-6.71	0.0000
		T_Range	19.19	3.45	5.57	0.0000
Biome 4	risk_MAT	(Intercept)	-11.15	1.73	-6.45	0.0000
		MAT	0.29	0.06	4.86	0.0000
		P_Dry	0.06	0.03	1.87	0.0705
	risk_MAP	(Intercept)	-1031.03	516.70	-2.00	0.0546
		MAP	1.38	0.31	4.42	0.0001
		MAT	-224.57	93.36	-2.41	0.0221
		P_Dry	-13.81	6.58	-2.10	0.0439
		T_Max	302.50	118.41	2.55	0.0156
		T_Range	-170.29	75.28	-2.26	0.0306
Biome 7	risk_MAT	(Intercept)	-19.01	1.42	-13.35	0.0000
		MAT	0.71	0.05	15.24	0.0000
		P_Dry	0.06	0.01	4.90	0.0000
		T_Range	0.05	0.01	3.66	0.0003
	risk_MAP	(Intercept)	-283.09	200.03	-1.42	0.1587
		MAP	0.53	0.06	9.36	0.0000
		MAT	-40.95	23.02	-1.78	0.0768
		P_Season	-2.26	0.81	-2.80	0.0057
		T_Max	72.00	22.29	3.23	0.0015
		T_Range	-40.60	10.16	-3.99	0.0001
Biome 12	risk_MAT	(Intercept)	-9.74	1.27	-7.68	0.0000
		P_Season	0.05	0.01	8.17	0.0000
		T_Max	0.17	0.04	4.66	0.0000
	risk_MAP	(Intercept)	-539.78	81.75	-6.60	0.0000
		MAP	0.96	0.05	19.72	0.0000
		MAT	22.93	4.18	5.48	0.0000
		P_Season	-0.92	0.31	-3.01	0.0030
Biome 13	risk_MAT	(Intercept)	-16.44	1.78	-9.26	0.0000
		MAT	0.46	0.07	6.90	0.0000

	P_Dry	-0.09	0.03	-3.36	0.0009
	T_Max	0.15	0.06	2.57	0.0109
	(Intercept)	-430.04	69.14	-6.22	0.0000
	MAP	1.15	0.04	27.45	0.0000
risk_MAP	**MAT**	-17.14	3.93	-4.36	0.0000
	P_Dry	4.17	1.20	3.47	0.0006
	T_Max	16.35	2.55	6.40	0.0000

Supplemental table S6. Coefficients from the best-supported linear regression models for climate-driven risk (MAT Risk and MAP Risk) against plant diversity metrics (S_R, S_D, F_D, F_R) at continental and biome scales. Shown are the estimated slope (estimate), standard error (std.error), t-value (statistic), and p-value for each predictor in the model. Models were selected based on the lowest AIC, and only the best-supported models are presented.

Scale	Response	Term	Estimate	Std error	Statistic	p-value
Continental	risk_MAT	(Intercept)	-1.64	0.09	-17.50	0.0000
	risk_MAP	(Intercept)	-65.79	20.01	-3.29	0.0011
		SR	-9.60	0.84	-11.44	0.0000
Biome 4	risk_MAT	(Intercept)	-6.53	0.84	-7.80	0.0000
		SR	0.04	0.03	1.64	0.1105
	risk_MAP	(Intercept)	-65.79	20.01	-3.29	0.0011
		SR	-9.60	0.84	-11.44	0.0000
Biome 7	risk_MAT	(Intercept)	0.33	0.11	3.09	0.0023
	risk_MAP	(Intercept)	204.46	54.41	3.76	0.0002
		FD	504.12	344.16	1.46	0.1448
		SR	9.69	1.91	5.08	0.0000
Biome 12	risk_MAT	(Intercept)	-3.27	0.31	-10.62	0.0000
		SR	0.03	0.01	2.85	0.0049
	risk_MAP	(Intercept)	354.88	107.14	3.31	0.0011
		FR	-392.63	138.64	-2.83	0.0052
		SR	5.30	0.88	6.05	0.0000
Biome 13	risk_MAT	(Intercept)	-1.05	0.53	-1.99	0.0477
		FD	6.64	2.65	2.50	0.0129
		SD	-2.16	0.94	-2.30	0.0226
	risk_MAP	(Intercept)	132.51	24.58	5.39	0.0000
		FD	433.62	124.27	3.49	0.0006
		SD	-242.05	47.84	-5.06	0.0000
		SR	4.39	0.82	5.33	0.0000